MyD88-Dependent Signaling for IL-15 Production Plays an Important Role in Maintenance of CD8$\alpha\alpha$ TCR$\alpha\beta$ and TCR$\gamma\delta$ Intestinal Intraepithelial Lymphocytes[1]

Qingsheng Yu,* Ce Tang,* Sun Xun,* Toshiki Yajima,* Kiyoshi Takeda,† and Yasunobu Yoshikai[2]*

Interaction between commensal bacteria and intestinal epithelial cells (i-ECs) via TLRs is important for intestinal homeostasis. In this study, we found that the numbers of CD8$\alpha\alpha$ TCR$\alpha\beta$ and TCR$\gamma\delta$ intestinal intraepithelial lymphocytes (i-IELs) were significantly decreased in MyD88-deficient (−/−) mice. The expression of IL-15 by i-ECs was severely reduced in MyD88$^{-/-}$ mice. Introduction of IL-15 transgene into MyD88$^{-/-}$ mice (MyD88$^{-/-}$ IL-15 transgenic mice) partly restored the numbers of CD8$\alpha\alpha$ TCR$\alpha\beta$ and TCR$\gamma\delta$ i-IELs. The i-IEL in irradiated wild-type (WT) mice transferred with MyD88$^{-/-}$ bone marrow (BM) cells had the same proportions of i-IEL as WT mice, whereas those in irradiated MyD88$^{-/-}$ mice transferred with WT BM cells showed significantly reduced proportions of CD8$\alpha\alpha$ TCR$\alpha\beta$ and TCR$\gamma\delta$ i-IELs, as was similar to the proportions found in MyD88$^{-/-}$ mice. However, irradiated MyD88$^{-/-}$ IL-15 transgenic mice transferred with WT BM cells had increased numbers of CD8$\alpha\alpha$ TCR$\alpha\beta$ and TCR$\gamma\delta$ subsets in the i-IEL. These results suggest that parenchymal cells such as i-ECs contribute to the maintenance of CD8$\alpha\alpha$ TCR$\alpha\beta$ and $\gamma\delta$ i-IELs at least partly via MyD88-dependent IL-15 production. *The Journal of Immunology,* 2006, 176: 6180–6185.

Intestinal intraepithelial lymphocytes (i-IELs),[3] which are located at the basolateral surfaces of intestinal epithelial cells (i-ECs), comprise unique T cell populations that include CD4$^-$/CD8$\alpha\alpha^+$ T cells expressing TCR$\alpha\beta$ or TCR$\gamma\delta$ and exhibit non-MHC-restricted cytotoxicity (1–3). The interaction of i-ECs and i-IELs through E-cadherin/integrin $\alpha_E\beta_7$ is important for the homing and maintenance of i-IELs (4). We previously showed that i-IELs recognized and eliminated effete i-ECs for homeostatic regulation of intestinal epithelia (5, 6). It has been reported that i-IELs, especially TCR$\gamma\delta$ i-IELs, play an important role in the regulation of generation and differentiation of i-ECs at crypts (7, 8). Taken together, results of previous studies suggest that mutual interaction of i-IELs and i-ECs is important for homeostasis of intestinal epithelia.

IL-15 is a cytokine that resembles IL-2 in its biological activity, stimulating macrophages (Mϕ), NK cells, TCR$\gamma\delta$ T cells, and B cells to proliferate, secrete cytokines, exhibit increased cytotoxicities, and produce Ab (9–12). IL-15 was found to be produced only by limited populations of cells, such as activated monocyte/Mϕ and epithelial cells, but not by activated T cells (13, 14). We previously reported that CD8$\alpha\alpha$ i-IELs proliferate preferentially in response to exogenous IL-15 (15). It has been shown that mice deficient in the *IL-15* or *IL-15R*α gene had reduced numbers of CD8$\alpha\alpha$ and/or TCR$\gamma\delta$ i-IELs (16, 17). Taken together, results of these studies suggest that IL-15 is involved in the development and proliferation of CD8$\alpha\alpha^+$ T cells in i-IELs.

It is widely accepted that intestinal microflorae play an important role in the maintenance of homeostasis of the intestinal microenvironment by inhibiting colonization by many pathogens and stimulating the growth of beneficial microorganisms. It has been reported recently that intestinal microflorae play an important role in maintaining i-ECs via TLRs (18). TLRs are a group of pattern recognition receptors that cooperate in recognizing a series of pathogens by binding to the pathogen-associated molecular patterns (19). After binding to their ligands, most of TLRs induce a series of intracellular signal transductions through MyD88, an adaptor protein for transcriptional activation of cytokine genes (20, 21). We and others previously reported that TLR signaling played important roles in activation of IL-15 transcription in LPS-stimulated Mϕ and virus-infected cell lines (22, 23). Thus, it is hypothesized that TLR signaling for IL-15 production via microflorae is involved in interaction of i-EC and i-IEL for maintaining homeostasis of the intestinal microenvironment.

In the present study, we found that the CD8$\alpha\alpha$ TCR$\alpha\beta$ and TCR$\gamma\delta$ i-IELs were selectively decreased in *MyD88*-deficient (−/−) mice, accompanied with impaired IL-15 expression by i-ECs. Introduction of IL-15 transgene into MyD88$^{-/-}$ mice was able to restore the numbers of CD8$\alpha\alpha$ TCR$\alpha\beta$ and TCR$\gamma\delta$ i-IELs, albeit partly. The experiments with bone marrow (BM) chimeras revealed that radioresistant parenchymal cells played an important role in MyD88-dependent maintenance of the i-IELs. We concluded that MyD88-dependent signaling was involved in interaction of i-EC and i-IEL for maintaining homeostasis of the intestinal microenvironment at least partly via IL-15 production.

*Division of Host Defense and †Division of Embryonic and Genetic Engineering, Medical Institute of Bioregulation, Kyushu University, Fukuoka, Japan

Received for publication September 12, 2005. Accepted for publication March 7, 2006.

The costs of publication of this article were defrayed in part by the payment of page charges. This article must therefore be hereby marked *advertisement* in accordance with 18 U.S.C. Section 1734 solely to indicate this fact.

[1] This work was supported in part by Grant-in-Aid for Scientific Research on Priority Areas, Japan Society for the Promotion of Science, and grants from the Japanese Ministry of Education, Science, and Culture (to Y.Y.), and Uehara Memorial Foundation (to Y.Y.).

[2] Address correspondence and reprint requests to Dr. Yasunobu Yoshikai, Division of Host Defense, Center for Prevention of Infectious Disease, Medical Institute of Bioregulation, Kyushu University, Fukuoka 812-8582, Japan. E-mail address: yoshikai@bioreg.kyushu-u.ac.jp

[3] Abbreviations used in this paper: i-IEL, intestinal intraepithelial lymphocyte; BM, bone marrow; i-EC, intestinal epithelial cell; Mϕ, macrophage; Tg, transgenic; WT, wild type.

0022-1767/06/$02.00

Materials and Methods

Animals

MyD88$^{-/-}$ and IL-15 transgenic (Tg) mice with C57BL/6 background were prepared as described previously (24, 25). MyD88$^{-/-}$/IL-15Tg mice were prepared by mating MyD88$^{-/-}$ and IL-15Tg mice and backcrossing them for three generations. Typing of MyD88$^{-/-}$ mice was performed by PCR with the primers described previously. C57BL/6NCrj mice used as wild-type (WT) controls were purchased from Charles River Laboratories. C57BL/6 Ly-5.1-congenic WT mice were obtained from The Jackson Laboratory. All of the mice were fed in a sterile, isolated room and used in experiments at ~8–10 wk of age. The animal experiments were approved by our institutional review committee according to a notice of the Prime Minister's Office of Japan (no. 6 of March 27, 1980) for the care and use of laboratory animals.

Preparation of i-IELs and i-ECs

Mice were sacrificed according to the relevant rules for animal usage. Peyer's patches and contents were removed from the small intestines of the mice, and small intestines were cut into pieces of <5 mm in length and stirred at 37°C for 30 min in medium 199 (Invitrogen Life Technologies) containing 10% FBS (Sigma-Aldrich). After stirring, the cells were passed through gauze to remove debris and coarse pieces and were centrifuged through a 25–40–75% discontinuous Percoll (Pharmacia) gradient that had been adjusted by 10× PBS at 940 × *g* for 20 min at 20°C in Multipurpose Refrigerated Centrifuge (Tomy). I-ECs and i-IELs are obtained at the interfaces of 25–40 and 40–75%, respectively. Cells were suspended in HBSS. A total of 10 μl of cell suspension was mixed with 90 μl of Turk's dye. A total of 10 μl of cell-Turks dye mixture was loaded onto a set of cell-counting plates, and the living cells were counted under a common optical microscope. The cells in each square were counted, and the total number of living cells was calculated by adjusting the number of cells in each square to the volume defined by the square and the whole volume of the cell suspension.

FACS analysis

Cells intended for FACS analysis were washed twice with FACS flow and suspended in 100 μl of FACS flow. Equal volumes of 2.4G2 (specific inhibitor for FcγR) were added to each sample and incubated on ice for 15 min. Cells of each sample were washed twice with FACS flow and suspended in 100 μl of FACS flow. Cells of each sample were stained with fluorescent dye- or biotin-conjugated Abs (PE-, FITC-, CyChrome (PE-Cy5)-, and biotin-conjugated anti-CD3, -CD4, -CD8α, -CD8β, -TCRβ, -TCRγδ, -CD45.1, -CD45.2 Abs (eBioscience)), which were finally diluted 200 times. To detect the cells specifically bound by biotin-conjugated Abs, the cells were incubated with allophycocyanin-conjugated streptavidin (eBioscience) after incubating the cells with biotin-conjugated Abs. All incubations were performed at 4°C for 30 min. The cells for each sample were washed by FACS flow twice after the incubation and suspended in ~500 μl of FACS flow. The samples were analyzed by FACSCalibur and interpreted by CellQuest software (BD Biosciences). Living lymphocytes were selected by gating on forward and side scattering. CD3$^+$, CD45.1$^+$, CD45.2$^+$, TCRαβ, and TCRγδ cells were selected by gating on histograms.

ELISA

Anti-CD3 mAb (clone number 145-2C11) was immobilized onto the bottom of each well of 96-well tissue culture plates (Falcon; BD Discovery Labware) overnight at 4°C at concentration of 50 μg/ml. MyD88$^{-/-}$ and WT i-IELs were cultured at concentration of 5 × 10^5 cells/well for 48 h at 37°C with 5% CO_2. Sandwich enzyme immunoassay was performed with the ELISA kits for IL-4, IL-10, and IFN-γ (R&D Systems). Recombinant mouse IL-4, IL-10, and IFN-γ were used as standard. The OD of each well was immediately read by Multiskan JX (ThermoLabsystems). The standard curve was drawn, and the concentration of each kind of cytokine was calculated according to the standard curve.

RT-PCR

Total RNA was extracted from i-ECs using TRIzol (Invitrogen Life Technologies). The first-strand cDNA was synthesized from 4 μg of RNA using 5× first-strand buffer, DTT, random primer, and SuperScript II RNase H-Reverse Transcriptase from Invitrogen Life Technologies and dNTP and RNase inhibitor from Toyobo Biochemicals for Life Science in a 20-μl system. The synthesized cDNA (2 μl) was amplified using PCR kit (Takara Bio) in a 50-μl system with primers described previously. The specific primers were as follows: β-actin sense, 5′-TTCTGCATCCTGTCAG CAAT-3′, and antisense, 5′-TAAAACGCAGCTCAGTAACAGTCCG-3′; primers for IL-15: sense from exon 1, 5′-GGAAGGCTGAGTTCCAC ATC-3′, and antisense from exon 5, 5′-AGGGAGACCTACACTGACAC-3′; sense from exon 3, 5′-GTTCTGGATGGATGGATGGCAGCT-3′, and antisense from exon 7, 5′-CTGTTTGCAAGGTAGAGCACG-3′ (26).

Generation of BM chimeras

BM hemopoietic cells were harvested from femurs and tibias of Ly-5.2$^+$MyD88$^{-/-}$ and Ly-5.1$^+$WT mice by lavaging the cavity of the bones with HBSS. The BM cells from Ly-5.2$^+$MyD88$^{-/-}$ mice were transferred to Ly-5.1$^+$WT mice. BM cells from Ly-5.1$^+$WT mice were transferred to Ly-5.2$^+$MyD88$^{-/-}$ mice or Ly-5.2$^+$MyD88$^{-/-}$ IL-15Tg mice. Recipients were irradiated with 1100 rad (11 Gy) of γ-ray in a single dose 3 h before the transfer with 5 × 10^6 BM cells through the tail vein. i-IELs derived from the donor in the BM chimeras were analyzed 8 wk after the BM transfer. i-IELs were gated by CD45.1 (Ly-5.1) or CD45.2 (Ly-5.2) according to their expression on the donor of the BM transfer by histogram to distinguish the donor-derived i-IELs from the host-derived i-IELs.

Statistical analysis

Student's *t* test was used to determine the statistically significant differences for cell counts between experimental groups. A value of $p < 0.05$ was taken as existence of statistically significant difference between experimental groups.

Results

CD8αα/TCRαβ and TCRγδ i-IELs were decreased in naive MyD88$^{-/-}$ mice

Differences between i-IEL subpopulations in naive MyD88$^{-/-}$ mice and WT mice were analyzed by FACS. Typical results are presented in Fig. 1*A*, and the mean number of each i-IEL subpopulation from five mice is summarized in Fig. 1*B*. Proportions of CD8αα/CD3$^+$ and TCRγδ/CD3$^+$ i-IELs were markedly decreased in MyD88$^{-/-}$ mice (Fig. 1*A*). MyD88$^{-/-}$ mice had significantly decreased numbers of CD8αα/CD3$^+$ and TCRγδ/CD3$^+$ i-IELs ($p < 0.01$; Fig. 1*B*). There were no significant differences in the numbers of CD8αβ/CD3$^+$ or TCRαβ/CD3$^+$ i-IELs between MyD88$^{-/-}$ and WT mice, although their proportions relatively were increased in MyD88$^{-/-}$ mice (Fig. 1, *A* and *B*). Nearly half of the TCRαβ$^+$ i-IELs expressed CD8αα in WT mice, while the proportion of CD8αα subpopulation in TCRαβ$^+$ i-IELs was decreased in MyD88$^{-/-}$ mice (Fig. 1*C*). In contrast, most of TCRγδ$^+$ i-IELs expressed CD8αα WT mice, and the proportion of CD8αα subpopulation was only slightly decreased in TCRγδ$^+$ i-IELs (Fig. 1*C*). Thus, CD8αα$^+$ subpopulation was selectively reduced in TCRαβ$^+$ i-IELs in MyD88$^{-/-}$ mice ($p < 0.05$; Fig. 1*D*), while TCRγδ$^+$ i-IELs were decreased in MyD88$^{-/-}$ mice regardless of CD8αβ ($p < 0.05$) or αα ($p < 0.01$; Fig. 1*D*).

Cytokine production by i-IEL in MyD88$^{-/-}$ mice

To investigate the qualitative difference of i-IEL in MyD88$^{-/-}$ mice from those in WT mice, we next examined IFN-γ, IL-4, and IL-10 production in the supernatant of i-IEL cultured with immobilized anti-CD3ε mAb by ELISA (Fig. 2). The concentrations of IL-10, IFN-γ, and IL-4 in the supernatant of cultured i-IEL of MyD88$^{-/-}$ mice were significantly increased as compared with WT mice ($p < 0.05$). Thus, these results suggest that i-IELs in MyD88$^{-/-}$ mice are comprised of larger numbers of i-IELs capable of producing higher levels of cytokines.

Introduction of IL-15 transgene can recover the number of CD8αα TCRαβ and TCRγδ i-IEL subpopulations in MyD88$^{-/-}$ mice

We and others have previously reported that IL-15 plays an important role in the development of CD8αα i-IEL and TCRγδ i-IEL (15–17). Furthermore, TLR signaling is important for transcriptional activation of *IL-15* gene (22, 23). These findings raise the

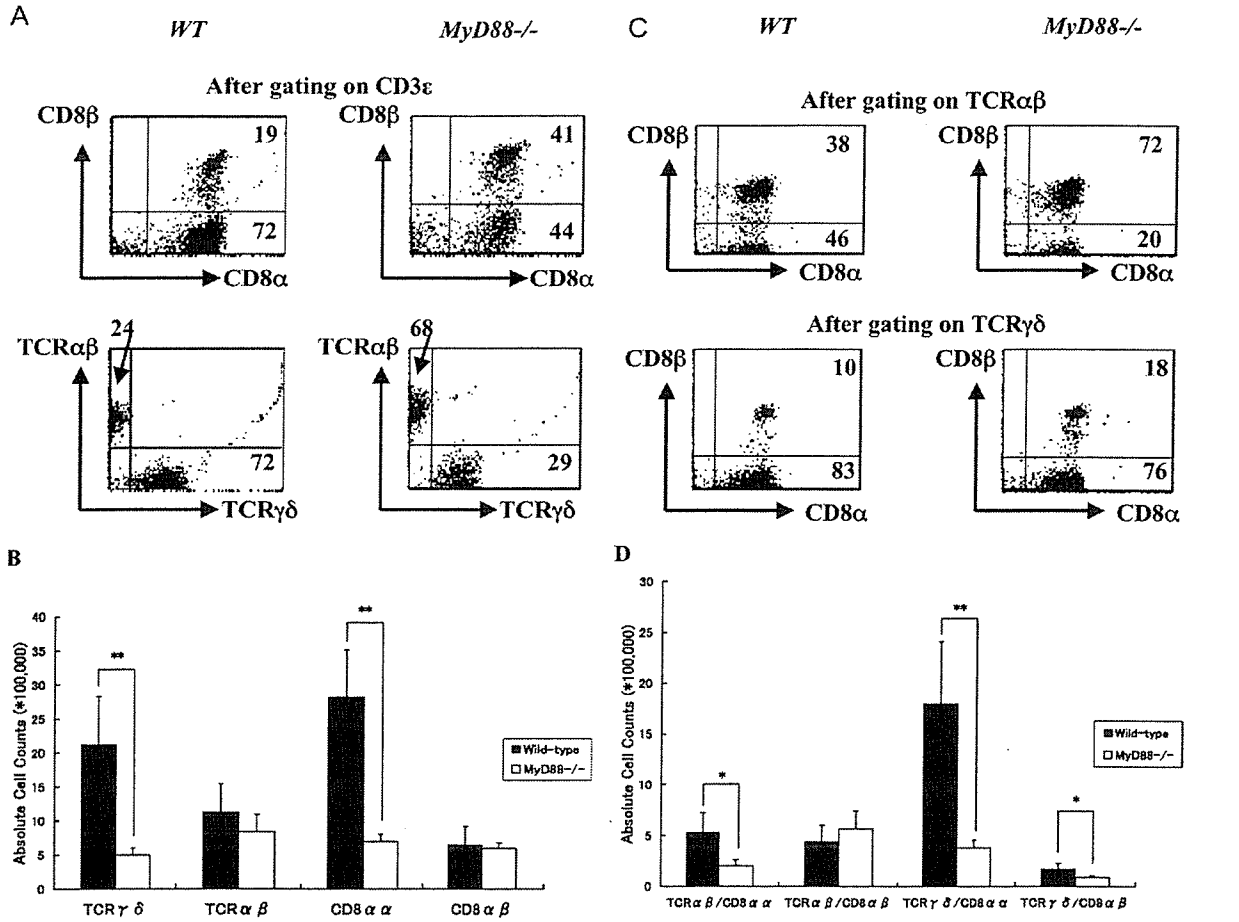

FIGURE 1. Analysis of i-IEL phenotypes of WT and MyD88$^{-/-}$ mice. *A*, Expression of CD8α and CD8β chains or TCR$\alpha\beta$ and TCR$\gamma\delta$ on CD3$^+$ i-IEL. Cells were stained with anti-CD3ε, anti-CD8α, and CD8β or TCR$\alpha\beta$ and TCR$\gamma\delta$ mAbs and positively gated by CD3ε. *B*, Absolute numbers of i-IEL subsets obtained from MyD88$^{-/-}$ mice. The absolute number of each subset was calculated by multiplying total number of i-IEL by the percentage of each subset. The data are shown as the mean of four mice ± SD. Significant differences compared with the value for WT mice are shown: **, $p < 0.01$. *C*, Expression of CD8α and CD8β chains on TCR$\alpha\beta$ or TCR$\gamma\delta$ i-IEL. Cells were stained with anti-TCR$\alpha\beta$ and anti-TCR$\gamma\delta$, anti-CD8α and anti-CD8β mAbs, and positively gated on TCR$\alpha\beta$ or TCR$\gamma\delta$. *D*, Absolute numbers of i-IEL subsets obtained from MyD88$^{-/-}$ mice. The absolute number of each subset was calculated by multiplying total number of i-IEL by the percentage of each subset. The data are shown as the mean of four mice ± SD. Significant differences compared with the value for WT mice are shown: *, $p < 0.05$; **, $p < 0.01$.

possibility that impairment of IL-15 production by radioresistant parenchymal cells such as i-EC may be responsible for decreased number of CD8$\alpha\alpha$ TCR$\alpha\beta$ and TCR$\gamma\delta$ i-IEL in MyD88$^{-/-}$ mice. To address this issue, we examined the expression of IL-15 mRNA by i-ECs of MyD88$^{-/-}$ mice using RT-PCR. We used two pairs of primers for IL-15: one specific for exons 3 and 7 and another specific for exons 1 and 5 (Fig. 3). The expression of IL-15 gene by i-ECs of MyD88$^{-/-}$ mice was severely reduced in both experiments using two kinds of primers (Fig. 3). These results strongly suggest that MyD88-dependent signaling is important for transcriptional activation of

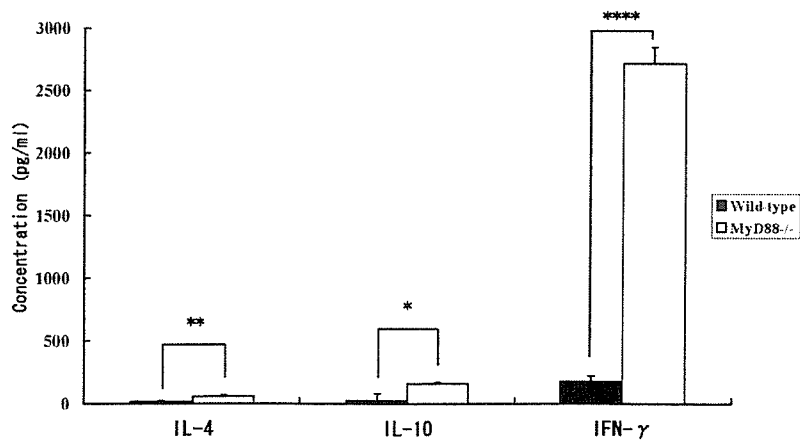

FIGURE 2. ELISA analysis of production of IL-4, IL-10, and IFN-γ by MyD88$^{-/-}$ i-IEL. Whole i-IEL (1×10^5) was cultured for 72 h with CD3ε mAb, and the culture supernatants were collected. The concentration of IFN-γ, IL-10, or IL-4 in the culture supernatants was determined by ELISA. The data are representative of three separate examinations using pooled cells from three mice and are shown as the mean of triplicate determinations ± SD. Significant differences compared with the value for WT mice are shown: *, $p < 0.05$; **, $p < 0.01$; ****, $p < 0.005$.

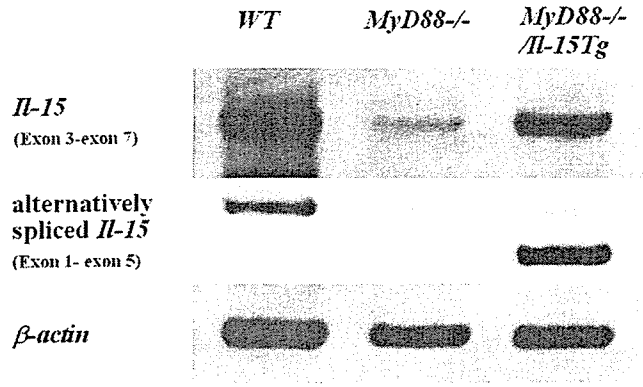

FIGURE 3. Expression of IL-15 mRNA by i-ECs from MyD88$^{-/-}$ and MyD88$^{-/-}$ IL-15Tg mice. IL-15 mRNA was reversely transcribed into first-strand cDNA. The first-strand cDNA was amplified using primers from exons 3 and 7 of IL-15 or using primers from exons 1 and 5 of IL-15. Two kinds of mRNA were shown. One was normal transcript comprising all exons. The other was alternatively spliced transcript that lacked exon 2, thereby 120 bp smaller than the normal transcript.

IL-15 gene in i-EC and consequently for development and/or maintenance of CD8$\alpha\alpha$ TCR$\alpha\beta$ and TCR$\gamma\delta$ i-IEL.

To address this possibility more directly, we introduced IL-15 transgene into MyD88$^{-/-}$ mice by crossing MyD88$^{-/-}$ mice with IL-15Tg mice carrying alternative spliced IL-15 cDNA lacking exon 2 under control of the H-2K promoter and Ig enhancer (24). As shown in Fig. 3, the expression level of IL-15 mRNA, as assessed with primers specific for exons 3 and 7, was increased in MyD88$^{-/-}$ IL-15Tg mice compared with MyD88$^{-/-}$ mice. To distinguish between IL-15 mRNA-derived endogenous gene and that from the transgene, we purposely used primers specific for exons 1 and 5 for RT-PCR. As shown in Fig. 3, IL-15 mRNA expressed by MyD88$^{-/-}$ IL-15Tg i-ECs was 120 bp smaller in size than those expressed by iEC of WT mice using primers for exons 1 and 5, indicating that the IL-15mRNA mainly derived from IL-15 transgene lacking exon 2.

We then analyzed the phenotype of i-IEL subpopulations in MyD88$^{-/-}$ IL-15Tg mice. As shown in Fig. 4, the proportions of CD8$\alpha\alpha$ TCR$\alpha\beta$ and TCR$\gamma\delta$ i-IELs were significantly increased in MyD88$^{-/-}$ IL-15Tg mice compared with MyD88$^{-/-}$ mice ($p < 0.05$ for TCR$\gamma\delta$ and $p < 0.01$ for CD8$\alpha\alpha$; Fig. 4, *A* and *B*). Thus, introduction of exogenous IL-15 by Tg manipulation was able to restore the CD8$\alpha\alpha$ TCR$\alpha\beta$ and TCR$\gamma\delta$ i-IELs in MyD88$^{-/-}$ mice.

Radioresistant host parenchymal cells are responsible for the change in i-IELs of MyD88$^{-/-}$ mice

TLRs are expressed not only by radio-susceptible hemopoietic cells such as Mϕ/dendritic cells, but also by radioresistant parenchymal cells such as epithelial cells (27). To determine whether hemopoietic or parenchymal cells are responsible for the development, differentiation, and maintenance of CD8$\alpha\alpha$/TCR$\alpha\beta$ and TCR$\gamma\delta$ i-IELs in MyD88$^{-/-}$ mice, we transferred BM cells for Ly-5.1$^+$WT mice and Ly-5.2$^+$MyD88$^{-/-}$ mice into lethally irradiated Ly-5.2$^+$MyD88$^{-/-}$ mice or Ly-5.2$^+$MyD88$^{-/-}$ IL-15Tg mice and Ly-5.1$^+$WT mice, respectively. As a result, we generated three types of BM chimera mice: the first type had parenchymal cells with functional MyD88 and hemopoietic cells deficient in MyD88 (Ly-5.2$^+$MyD88$^{-/-}$ mice as donors and Ly-5.1$^+$WT mice as recipients); the second type had parenchymal cells deficient in MyD88 and hemopoietic cells with functional MyD88 (Ly-5.1$^+$WT mice as BM donor and Ly-5.2$^+$MyD88$^{-/-}$ mice as recipients); and the third type had parenchymal cells deficient in MyD88, but carrying IL-15 transgene and hemopoietic cells with functional MyD88 (Ly-5.1$^+$WT mice as BM donor and Ly-5.2$^+$MyD88$^{-/-}$ IL-15Tg mice as recipients). Consistent with results obtained in our previous studies (28), hemopoietic cells were almost completely replaced by donor-derived hemopoietic cells in i-IELs by 8 wk after BM cell transfer in both types of BM chimera mice (data not shown). We analyzed the phenotypes of donor-derived CD8$\alpha\alpha$/CD3$^+$, CD8$\alpha\beta$/CD3$^+$, TCR$\alpha\beta$/CD3$^+$, and TCR$\gamma\delta$/CD3$^+$ i-IELs of BM chimera mice at 8 wk after BM transfer (Fig. 5). The Ly-5.2$^+$MyD88$^{-/-}$ donor-derived i-IELs in BM chimera mice with Ly-5.1$^+$WT parenchymal cells had the same proportions of CD8$\alpha\alpha$/CD3$^+$ and TCR$\gamma\delta$/CD3$^+$ i-IELs as WT mice (Fig. 5). The Ly-5.1$^+$WT donor-derived i-IELs in BM chimera mice with Ly-5.2$^+$MyD88$^{-/-}$ parenchymal cells showed significantly reduced proportions of CD8$\alpha\alpha$/CD3$^+$ i-IEL ($p < 0.05$) and TCR$\gamma\delta$/CD3$^+$ i-IELs ($p < 0.01$), as was similar to the proportions found in MyD88$^{-/-}$ mice, whereas the Ly-5.1$^+$WT donor-derived i-IELs in BM chimera mice with Ly-5.2$^+$MyD88$^{-/-}$ IL-15Tg parenchymal cells showed significantly increased numbers of CD8$\alpha\alpha$/CD3$^+$ i-IEL ($p < 0.05$) and

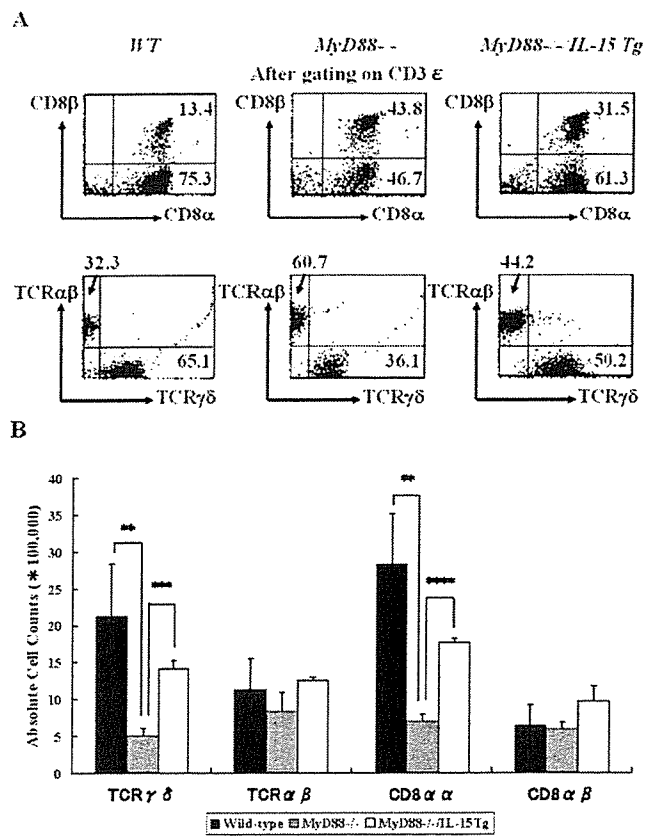

FIGURE 4. Analysis of i-IEL phenotypes of MyD88$^{-/-}$ mice and MyD88$^{-/-}$ IL-15Tg mice. *A*, Expression of CD8α and CD8β chains on CD3$^+$ i-IEL. Cells were stained with anti-CD3ε, anti-CD8α, and anti-CD8β mAbs and positively gated by CD3ε. Expression of TCR$\alpha\beta$ or TCR$\gamma\delta$ i-IEL on CD3$^+$ i-IEL. Cells were stained with anti-CD3ε, anti-TCR$\alpha\beta$, and anti-TCR$\gamma\delta$ mAbs, and positively gated by CD3ε. *B*, Absolute numbers of i-IEL subsets obtained from MyD88$^{-/-}$ mice and MyD88$^{-/-}$ IL-15Tg mice. The absolute number of each subset was calculated by multiplying total number of i-IEL by the percentage of each subset. The data are shown as the mean of four mice ± SD. Significant differences compared with the value for WT mice are shown: **, $p < 0.01$. Significant differences compared with the value for MyD88$^{-/-}$ mice are shown: ***, $p < 0.05$; ****, $p < 0.01$.

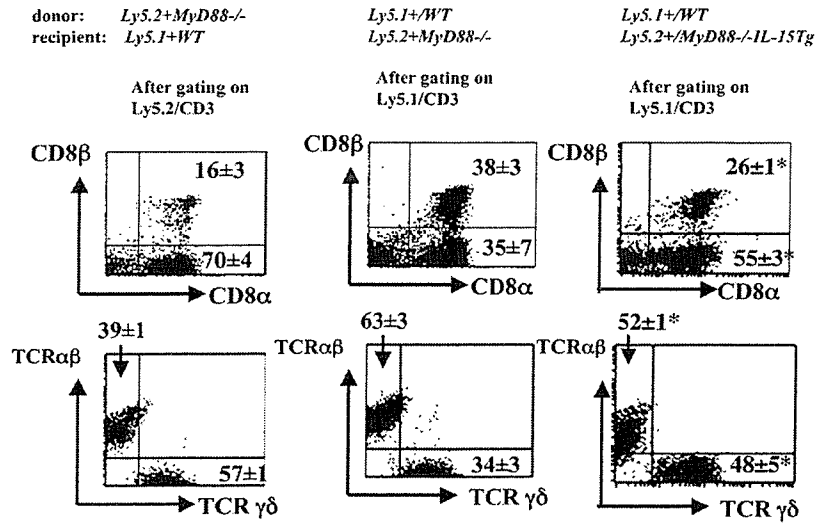

FIGURE 5. Analysis of phenotypes of the donor-derived CD3$^+$ i-IELs in BM chimera mice. Ly-5.1$^+$WT mice and Ly-5.2$^+$MyD88$^{-/-}$ or Ly-5.2$^+$MyD88$^{-/-}$ IL-15Tg mice transferred with Ly-5.2$^+$MyD88$^{-/-}$ BM cells and Ly-5.1$^+$WT BM cells after 1100 rad of gamma ray irradiation, respectively. i-IELs derived from the donor in the BM chimeras were analyzed 8 wk after the BM transfer. i-IEL were stained with anti-CD3ε, anti-CD8α, or anti-TCR$\alpha\beta$, anti-CD8β, or anti-TCR$\gamma\delta$, and anti-Ly-5.1 or anti-Ly-5.2 mAbs and gated on CD3 and Ly-5.1- or Ly-5.2-positive cells. The data are shown as the mean of four mice ± SD. Significant differences compared with the value for irradiated MyD88$^{-/-}$ mice transferred with WT BM cells are shown: *, $p < 0.05$.

TCR$\gamma\delta$/CD3$^+$ i-IELs ($p < 0.05$). These results suggest that the changes in the proportions of CD8$\alpha\alpha$ TCR$\alpha\beta$ and TCR$\gamma\delta$ i-IELs in MyD88$^{-/-}$ mice essentially depend on the deficiency of MyD88 in radioresistant parenchymal cells rather than on hemopoietic cells, and that introduction of exogenous IL-15 in the parenchymal cells by Tg manipulation was able to restore the CD8$\alpha\alpha$ TCR$\alpha\beta$ and TCR$\gamma\delta$ i-IELs.

Discussion

Several cytokines and hormones, such as c-*kit*, thymotrophin-releasing hormones, IL-7, and IL-15, are known to be involved in development and maintenance of CD8$\alpha\alpha$ i-IEL (15–17, 29, 30). Schluns et al. (31) proved that the development of CD8$\alpha\alpha$ i-IEL subset completely depended on the expression of IL-15 and IL-15Rα of parenchymal cells. We found that MyD88-dependent signaling in radioresistant host parenchymal cells played an important role in development of CD8$\alpha\alpha$ TCR$\alpha\beta$ and TCR$\gamma\delta$ i-IELs, and the signaling was essential in transcriptional activation of IL-15 in i-EC. It is most likely that i-EC contribute to development and maintenance of CD8$\alpha\alpha$ TCR$\alpha\beta$ and TCR$\gamma\delta$ i-IEL via IL-15 production, although the possibility is not excluded that other parenchymal cells might be involved in IL-15 production. We and others previously reported that transcriptional factors, including NF-κB, played important roles in transcriptional activation of IL-15 in LPS-stimulated Mϕ and virus-infected cell lines (22, 23). MyD88 is a very important adaptor in the pathway of the signal transduction of most TLRs, which activate NF-κB (19, 21, 24). Thus, MyD88-dependent signaling for IL-15 production from interaction between commensal bacteria and i-ECs via TLRs may play an important role in development and maintenance of CD8$\alpha\alpha$/TCR$\alpha\beta$ and TCR$\gamma\delta$ i-IELs. Our data showed that the proportions of CD8$\alpha\alpha$ TCR$\alpha\beta$ and TCR$\gamma\delta$ i-IELs were not completely restored to the normal level of WT mice after introduction of IL-15 transgene into MyD88$^{-/-}$ mice. This may be because the expression of IL-15 in MyD88$^{-/-}$ IL-15Tg mice did not reach the normal level. Alternatively, some subpopulations in CD8$\alpha\alpha$ TCR$\alpha\beta$ and TCR$\gamma\delta$ i-IELs may depend for their development and maintenance on factors other than IL-15, which are also induced by MyD88-dependent signaling. The factors may remain at low level, resulting in incomplete restoration of the i-IEL in MyD88$^{-/-}$ IL-15Tg mice. Additional experiments for V repertoire and surface markers are needed to clarify this possibility.

Murine i-IELs consist of approximately equal amounts of TCR$\alpha\beta$ and TCR$\gamma\delta$ i-IELs and unique populations bearing CD8 homodimeric α-chains as well as those bearing CD8 heterodimeric α- and β-chains (32, 33). i-IELs produce a variety of cytokines, including Th1-type cytokines, Th2-type cytokines (34), and immunosuppressive cytokines such as TGF-β and IL-10 (35). i-IELs are thought to play important roles in the helper function for local IgA response and homeostasis of i-ECs through production of cytokines such as TGF-β (36). i-IELs also exhibit non-MHC-restricted cytotoxicity via serine esterase-dependent and Fas/Fas ligand-dependent mechanisms that provide surveillance against infected cells, premalignant cells, and effete cells (5–6). TCR$\gamma\delta^{-/-}$ mice showed impaired development of villi (7, 37), suggesting that TCR$\gamma\delta$ i-IELs play an important role in homeostasis of i-EC differentiation. It has been reported that a significant fraction of i-IELs such as TCR$\gamma\delta$ i-IELs and CD8$\alpha\alpha$ i-IELs is thought to down-regulate excessive inflammation caused by infection and autoimmunity (8, 38, 39). In the present study, we found that whole i-IEL in MyD88$^{-/-}$ mice produced the larger amounts of IFN-γ upon TCR triggering than those in WT mice. It is most likely that the increased cytokine production simply reflects the relatively increased number of CD8$\alpha\beta$ TCR$\alpha\beta$ i-IEL in MyD88$^{-/-}$ mice. However, it is also possible that MyD88-dependent i-IEL populations may suppress the function of CD8$\alpha\beta$ TCR$\alpha\beta$ i-IEL upon TCR triggering via their suppressive activities.

Rakoff-Nahoum et al. (18) have reported recently that MyD88$^{-/-}$ mice showed a defect in steady state intestinal epithelial homeostasis, resulting in high susceptibility to intestinal injury induced by dextran disulfide sodium. These results suggest that MyD88-dependent TLR signaling in i-ECs plays an important role in the homeostasis of i-ECs. They also reported increase in count of proliferating i-ECs in MyD88$^{-/-}$ mice and reduced levels of cytoprotective cytokines such as IL-6 and KC/CXCL1 and cytoprotective protein, heat shock protein, produced by i-ECs in MyD88$^{-/-}$ mice. They speculated that the direct stimulation of i-ECs by intestinal microflorae via MyD88-dependnet TLR signaling induces cytoprotective cytokines and proteins, including IL-6 and heat shock protein, which result in steady state intestinal epithelial homeostasis. We previously reported that CD8$\alpha^{-/-}$ mice showed high susceptibility to 5-fluorouracil-induced intestinal injury (40), suggesting that CD8$\alpha\alpha$ i-IELs are important for intestinal homeostasis. Therefore, we suggest that impairment of development, differentiation, and maintenance of CD8$\alpha\alpha$ and TCR$\gamma\delta$ i-IELs in MyD88$^{-/-}$ mice accounts at least partially for the defect in steady state intestinal epithelial homeostasis and susceptibility to intestinal injury.

In summary, we found that MyD88-dependent signaling is important for the development and maintenance of CD8$\alpha\alpha$ TCR$\alpha\beta$ and TCR$\gamma\delta$ i-IELs in mice. Experiments with BM chimera mice demonstrated that MyD88-dependent signaling in radioresistant host parenchymal cells is important in keeping the number of the i-IEL populations. The expression level of IL-15 was greatly reduced in i-ECs of MyD88$^{-/-}$ mice, and introduction of IL-15 transgene in MyD88$^{-/-}$ mice restored the numbers of CD8$\alpha\alpha$ TCR$\alpha\beta$ and TCR$\gamma\delta$ i-IELs in MyD88$^{-/-}$ mice. These results suggest that MyD88-dependent signaling for IL-15 production from interaction between commensal bacteria and i-ECs via TLRs plays an important role in maintenance of the number of CD8$\alpha\alpha$/TCR$\alpha\beta$ and TCR$\gamma\delta$ i-IELs.

Acknowledgments

We express our gratitude to Y. Kobayashi and K. Kaneda for their excellent technical assistance.

Disclosures

The authors have no financial conflict of interest.

References

1. Guy-Grand, D., and P. Vassalli. 1993. Gut intraepithelial T lymphocytes. *Curr. Opin. Immunol.* 5: 247–252.
2. Klein, J. R. 2004. T-cell activation in the curious world of the intestinal intraepithelial lymphocyte. *Immunol. Res.* 30: 327–337.
3. Cheroutre, H. 2004. Starting at the beginning: new perspectives on the biology of mucosal T cells. *Annu. Rev. Immunol.* 22: 217–246.
4. Yoshikai, Y. 1999. The interaction of intestinal epithelial cells and intraepithelial lymphocytes in host defense. *Immunol. Res.* 20: 219–235.
5. Inagaki-Ohara, K., H. Nishimura, T. Sakai, D. H. Lynch, and Y. Yoshikai. 1997. Potential for involvement of Fas antigen/Fas ligand interaction in apoptosis of epithelial cells by intraepithelial lymphocytes in murine small intestine. *Lab. Invest.* 77: 421–429.
6. Sakai, T., Y. Kimura., K. Inagaki-Ohara, K. Kusugami, D. H. Lynch, and Y. Yoshikai. 1997. Fas-mediated cytotoxicity by host intestinal intraepithelial lymphocytes is involved in the enteropathy during acute graft-vs.-host disease. *Gastroenterology* 113: 168–174.
7. Komano, H., Y. Fujiura, M. Kawaguchi, S. Matsumoto, Y. Hashimoto, S. Obana, P. Mombaerts, S. Tonegawa, H. Yamamoto, and S. Itohara. 1995. Homeostatic regulation of intestinal epithelia by intraepithelial $\gamma\delta$ T cells. *Proc. Natl. Acad. Sci. USA* 92: 6147–6151.
8. Hayday, A., and R. Tigelaar. 2003. Immunoregulation in the tissues by γ/δ T cells. *Nat. Rev. Immunol.* 3: 233–242.
9. Grabstein, K. H., J. Eisenman, K. Shanebeck, C. Rauch, S. Srinivasan, V. Fung, C. Beers, J. Richardson, M. A. Schoenborn, M. Ahdieh, et al. 1994. Cloning of a T cell growth factor that interacts with the β chain of the interleukin-2 receptor. *Science* 264: 965–968.
10. Bamford, R. N., A. J. Grant, J. D. Burton, C. Peters, G. Kurys, C. K. Goldman, J. Brennan, E. Roessler, and T. A. Waldmann. 1994. The interleukin (IL) 2 receptor β chain is shared by IL-2 and a cytokine, provisionally designated IL-T, that stimulates T-cell proliferation and the induction of lymphokine-activated killer cells. *Proc. Natl. Acad. Sci. USA* 91: 4940–4944.
11. Waldmann, T. A., and Y. Tagaya. 1999. The multifaceted regulation of interleukin-15 expression and the role of this cytokine in NK cell differentiation and host response to intracellular pathogens. *Annu. Rev. Immunol.* 17: 19–49.
12. Fehniger, T. A., and M. A. Caligiuri. 2001. Interleukin 15: biology and relevance to human disease. *Blood* 97: 14–32.
13. Reinecker, H. C., R. P. MacDermott, S. Mirau, A. Dignass, and D. K. Podolsky. 1996. Intestinal epithelial cells both express and respond to interleukin 15. *Gastroenterology* 111: 1706–1713.
14. Hirose, K., H. Suzuki, H. Nishimura, A. Mitani, J. Washizu, T. Matsuguchi, and Y. Yoshikai. 1998. Interleukin-15 may be responsible for early activation of intestinal intraepithelial lymphocytes after oral infection with *Listeria monocytogenes* in rats. *Infect. Immun.* 66: 5677–5683.
15. Inagaki-Ohara, K., H. Nishimura, A. Mitani, and Y. Yoshikai. 1997. Interleukin-15 preferentially promotes the growth of intestinal intraepithelial lymphocytes bearing $\gamma\delta$ T cell receptor in mice. *Eur. J. Immunol.* 27: 2885–2891.
16. Lodolce, J. P., D. L. Boone, S. Chai, R. E. Swain, T. Dassopoulos, S. Trettin, and A. Ma. 1998. IL-15 receptor maintains lymphoid homeostasis by supporting lymphocyte homing and proliferation. *Immunity* 9: 669–676.
17. Kennedy, M. K., M. Glaccum, S. N. Brown, E. A. Butz, J. L. Viney, M. Embers, N. Matsuki, K. Charrier, L. Sedger, C. R. Willis, et al. 2000. Reversible defects in natural killer and memory CD8 T cell lineages in interleukin 15-deficient mice. *J. Exp. Med.* 191: 771–780.
18. Rakoff-Nahoum, S., J. Paglino, F. Eslami-Varzaneh, S. Edberg, and R. Medzhitov. 2004. Recognition of commensal microflora by Toll-like receptors is required for intestinal homeostasis. *Cell* 118: 229–241.
19. Takeda, K., T. Kaisho, and S. Akira. 2003. Toll-like receptors. *Annu. Rev. Immunol.* 21: 335–376.
20. Kawai, T., O. Adachi, T. Ogawa, K. Takeda, and S. Akira. 1999. Unresponsiveness of MyD88-deficient mice to endotoxin. *Immunity* 11: 115–122.
21. Beutler, B. 2004. Inferences, questions and possibilities in Toll-like receptor signaling. *Nature* 430: 257–263.
22. Washizu, J., H. Nishimura, N. Nakamura, Y. Nimura, and Y. Yoshikai. 1998. The NF-κB binding site is essential for transcriptional activation of the IL-15 gene. *Immunogenetics* 48: 1–7.
23. Azimi, N., K. Brown, R. N. Bamford, Y. Tagaya, U. Siebenlist, and T. A. Waldmann. 1998. Human T cell lymphotropic virus type I Tax protein trans-activates interleukin 15 gene transcription through an NF-κB site. *Proc. Natl. Acad. Sci. USA* 95: 2452–2457.
24. Adachi, O., T. Kawai, K. Takeda, M. Matsumoto, H. Tsutsui, M. Sakagami, K. Nakanishi, and S. Akira. 1998. Targeted disruption of the *MyD88* gene results in loss of IL-1- and IL-18-mediated function. *Immunity* 9: 143–150.
25. Nishimura, H., T. Yajima, Y. Naiki, H. Tsunobuchi, M. Umemura, K. Itano, T. Matsuguchi, M. Suzuki, P. S. Ohashi, and Y. Yoshikai. 2000. Differential roles of interleukin 1 mRNA isoforms generated by alternative splicing in immune responses in vivo. *J. Exp. Med.* 191: 157–170.
26. Nishimura, H., J. Washizu, N. Nakamura, A. Enomoto, and Y. Yoshikai. 1998. Translational efficiency is up-regulated by alternative exon in murine IL-15 mRNA. *J. Immunol.* 160: 936–942.
27. Abreu, M. T., M. Fukata, and M. Arditi. 2005. TLR signaling in the gut in health and disease. *J. Immunol.* 174: 4453–4460.
28. Yoshikai, Y., M. Ogimoto, G. Matsuzaki, and K. Nomoto. 1990. Bone marrow-derived cells are essential for intrathymic deletion of self-reactive T cells in both the host and donor-derived thymocytes of fully allogeneic bone marrow chimeras. *J. Immunol.* 145: 505–509.
29. Laky, K., L. Lefrancois, E. G. Lingenheld, H. Ishikawa, J. M. Lewis, S. Olson, K. Suzuki, R. E. Tigelaar, and L. Puddington. 2000. Enterocyte expression of interleukin 7 induces development of γ/δ T cells and Peyer's patches. *J. Exp. Med.* 191: 1569–1580.
30. Wang, J., M. Whetsell, and J. R. Klein. 1997. Local hormone networks and intestinal T cell homeostasis. *Science* 275: 1937–1939.
31. Schluns, K. S., E. C. Nowak, A. Cabrera-Hernandez, L. Puddington, L. Lefranccois, and H. L. Aguila. 2004. Distinct cell types control lymphoid subset development by means of IL-15 and IL-15 receptor α expression. *Proc. Natl. Acad. Sci. USA* 101: 5616–5621.
32. Bonneville, M., C. A. Janeway, K. Ito, W. Haser, I. Ishida, N. Nakanishi, and S. Tonegawa. 1988. Intestinal intraepithelial lymphocytes are a distinct set of $\gamma\delta$ T cells. *Nature* 336: 479–481.
33. Guy-Grand, D., N. Cerf-Bensussan, B. Malissen, M. Malassis-Seris, C. Briottet, and P. Vassalli. 1991. Two gut intraepithelial CD8$^+$ lymphocyte populations with different T cell receptors: a role for the gut epithelium in T cell differentiation. *J. Exp. Med.* 173: 471–481.
34. Taguchi, T., W. K. Aicher, K. Fujihashi, M. Yamamoto, J. R. McGhee, J. A. Bluestone, and H. Kiyono. 1991. Novel function for intestinal intraepithelial lymphocytes: murine CD3$^+$, γ/δ TCR$^+$ T cells produce IFN-γ and IL-5. *J. Immunol.* 147: 3736–3744.
35. Fujihashi, K., M. Yamamoto, J. R. McGhee, K. W. Beagley, and H. Kiyono. 1993. Function of $\alpha\beta$ TCR$^+$ intestinal intraepithelial lymphocytes: Th1- and Th2-type cytokine production by CD4$^+$CD8$^-$ and CD4$^+$CD8$^+$ T cells for helper activity. *Int. Immunol.* 5: 1473–1481.
36. Yamamoto, M., K. Fujihashi, K. W. Beagley, J. R. McGhee, and H. Kiyono. 1993. Cytokine synthesis by intestinal intraepithelial lymphocytes: both γ/δ T cell receptor-positive and α/β T cell receptor-positive T cells in the G_1 phase of cell cycle produce IFN-γ and IL-5. *J. Immunol.* 150: 106–114.
37. Yang, H., P. A. Antony, B. E. Wildhaber, and D. H. Teitelbaum. 2004. Intestinal intraepithelial lymphocyte $\gamma\delta$-T cell-derived keratinocyte growth factor modulates epithelial growth in the mouse. *J. Immunol.* 172: 4151–4158.
38. Das, G., M. M. Augustine, J. Das, K. Bottomly, P. Ray, and A. Ray. 2003. An important regulatory role for CD4$^+$CD8$^+$ $\alpha\alpha$ T cells in the intestinal epithelial layer in the prevention of inflammatory bowel disease. *Proc. Natl. Acad. Sci. USA* 100: 5324–5329.
39. Roberts, S. J., A. L. Smith, A. B. West, L. Wen, R. C. Findly, M. J. Owen, and A. C. Hayday. 1996. T-cell $\alpha\beta^+$ and $\gamma\delta^+$ deficient mice display abnormal but distinct phenotypes toward a natural, widespread infection of the intestinal epithelium. *Proc. Natl. Acad. Sci. USA* 93: 11774–11779.
40. Itoh, N., H. Nishimura, T. Matsuguchi, T. Yajima, Y. Mokuno, T. Hiromatsu, Y. Nimura, and Y. Yoshikai. 2002. CD8 α-deficient mice are highly susceptible to 5-fluorouracil-induced lethality. *Clin. Diagn. Lab. Immunol.* 9: 550–557.

Essential Role of IκB Kinase α in Thymic Organogenesis Required for the Establishment of Self-Tolerance[1]

Dan Kinoshita,* Fumiko Hirota,[‡] Tsuneyasu Kaisho,[§] Michiyuki Kasai,[¶] Keisuke Izumi,[†] Yoshimi Bando,[†] Yasuhiro Mouri,[‡] Akemi Matsushima,[‡] Shino Niki,[‡] Hongwei Han,[‡] Kiyotaka Oshikawa,[‡] Noriyuki Kuroda,[‡] Masahiko Maegawa,* Minoru Irahara,* Kiyoshi Takeda,[‖] Shizuo Akira,[#] and Mitsuru Matsumoto[2‡]

IκB kinase (IKK) α exhibits diverse biological activities through protein kinase-dependent and -independent functions, the former mediated predominantly through a noncanonical NF-κB activation pathway. The in vivo function of IKKα, however, still remains elusive. Because a natural strain of mice with mutant NF-κB-inducing kinase (NIK) manifests autoimmunity as a result of disorganized thymic structure with abnormal expression of Rel proteins in the thymic stroma, we speculated that the NIK-IKKα axis might constitute an essential step in the thymic organogenesis that is required for the establishment of self-tolerance. An autoimmune disease phenotype was induced in athymic *nude* mice by grafting embryonic thymus from IKKα-deficient mice. The thymic microenvironment that caused autoimmunity in an IKKα-dependent manner was associated with defective processing of NF-κB2, resulting in the impaired development of thymic epithelial cells. Thus, our results demonstrate a novel function for IKKα in thymic organogenesis for the establishment of central tolerance that depends on its protein kinase activity in cooperation with NIK. *The Journal of Immunology,* **2006, 176: 3995–4002.**

The transcription factor NF-κB plays an important role in the regulation of innate immunity, stress responses, inflammation, and the inhibition of apoptosis (1, 2). The activity of NF-κB is tightly regulated through the IκB kinase (IKK)[3] complex, which consists of two catalytic subunits (IKKα and IKKβ) and a regulatory subunit (IKKγ) (2). IKKα has been shown to be phosphorylated by NF-κB-inducing kinase (NIK) (3), which is structurally related to MEK kinase (4). Many aspects of the in vivo function of these key players have been elucidated by the use of both gene-targeted mice and natural mutant mice (2). The alymphoplasia (*aly*) strain of mice carries a natural mutation of the NIK gene (5, 6) in which a G855R substitution in the C terminus of the protein results in inability to bind to IKKα (7). We have demonstrated previously that a defective NIK-IKKα axis downstream of lymphotoxin (LT) βR, a receptor essential for secondary lymphoid organogenesis (8), is responsible for the abnormal development of secondary lymphoid organs in *aly* mice (7, 9).

In addition to its essential role in secondary lymphoid organogenesis, we have demonstrated recently that NIK is required in the thymic stroma for the organization of the thymic microenvironment (10). Abnormal thymic organogenesis in the absence of normal NIK accounts for the autoimmune disease phenotype seen in *aly* mice, which is characterized by chronic inflammatory changes in several organs, including the liver, pancreas, salivary gland, and lacrimal gland (5, 10). Because breakdown of self-tolerance is considered to be the key event responsible for the autoimmune disease process, and establishment of self-tolerance primarily depends on physical contact between thymocytes and thymic stroma (11), characterization of the stromal elements involved may contribute to the development of a therapeutic approach to many autoimmune diseases.

Medullary thymic epithelial cells (mTECs) play pivotal roles in the cross talk between developing thymocytes and thymic stroma (12). Elimination of autoreactive T cells (negative selection) and/or production of immunoregulatory T cells (Tregs) are most likely mediated by a set of self Ags expressed on mTECs (13, 14). In fact, gene expression studies have demonstrated that mTECs are a specialized cell type in which promiscuous expression of a broad range of tissue-specific Ag (TSA) genes is an autonomous property (15). Studies on mice with autoimmune phenotypes resulting from an abnormal thymic microenvironment have provided useful insights into this mechanism. Autoimmune regulator (Aire)-deficient mice have mTECs with reduced expression of many, but not all, TSAs, but have apparently normal thymic structure (16, 17). These results suggest that Aire regulates transcription of TSAs within developed mTECs without influencing the development of these cells. In contrast, reduced expression of TSAs (and Aire) in the thymus from NIK mutant mice is associated with impaired development of mTECs (10); $NIK^{aly/aly}$

*Department of Obstetrics and Gynecology and [†]Department of Molecular and Environmental Pathology, Institute of Health Biosciences, University of Tokushima Graduate School, Tokushima, Japan; [‡]Division of Molecular Immunology, Institute for Enzyme Research, University of Tokushima, Tokushima, Japan; [§]Laboratory for Host Defense, Research Center for Allergy and Immunology, Kanagawa, Japan; [¶]Division of Bacterial and Blood Products, National Institute of Infectious Disease, Tokyo, Japan; [‖]Division of Embryonic and Genetic Engineering, Medical Institute of Bioregulation, Kyushu University, Fukuoka, Japan; and [#]Department of Host Defense, Research Institute for Microbial Diseases, Osaka University, Osaka, Japan

Received for publication July 19, 2005. Accepted for publication January 26, 2006.

The costs of publication of this article were defrayed in part by the payment of page charges. This article must therefore be hereby marked *advertisement* in accordance with 18 U.S.C. Section 1734 solely to indicate this fact.

[1] This work was supported in part by Special Coordination Funds of the Ministry of Education, Culture, Sports, Science, and Technology, the Japanese Government, and by Grant-in-Aid for Scientific Research from the Ministry of Education, Culture, Sports, Science, and Technology, the Japanese Government (17047028 and 17390291).

[2] Address correspondence and reprint requests to Dr. Mitsuru Matsumoto, Division of Molecular Immunology, Institute for Enzyme Research, University of Tokushima, 3-18-15 Kuramoto, Tokushima 770-8503, Japan. E-mail address: mitsuru@ier.tokushima-u.ac.jp

[3] Abbreviations used in this paper: IKK, IκB kinase; Aire, autoimmune regulator; *aly*, alymphoplasia; CAT-S, cathepsin S; CRP, C-reactive protein; 2-DG, 2′-deoxyguanosine; FABP, fatty acid-binding protein; HPRT, hypoxanthine phosphoribosyltransferase; LT, lymphotoxin; mTEC, medullary thymic epithelial cell; NIK, NF-κB-inducing kinase; SP1, salivary protein 1; TEC, thymic epithelial cell; TRAF, TNFR-associated factor; Treg, immunoregulatory T cell; TSA, tissue-specific Ag; UEA, *Ulex europaeus* agglutinin; Ep-CAM, epithelial cell adhesion molecule; GAD67, glutamic acid decarboxylase 67.

0022-1767/06/$02.00

mice lack *Ulex europaeus* (UEA)-1$^+$ mTECs and have reduced numbers of ER-TR5$^+$ mTECs. Although these results are consistent with the idea that NIK affects TSA expression in the thymus through a developmental effect on mTECs, it is not clear whether NIK has any significant roles in the transcription of TSA genes within these cells, as suggested for Aire.

Initial studies of mice deficient in IKKα have unveiled an unexpected function of IKKα for the development of limbs and skin (18, 19). Subsequent studies have revealed a two-dimensional role for IKKα, which possesses both protein kinase-dependent and protein kinase-independent functions. It has been demonstrated that kinase activity is required for lymphoid organogenesis (7, 20), B cell development and function (21), and mammary gland development (22). In contrast, kinase-independent activity is required for epidermal keratinocyte differentiation and skeletal and craniofacial morphogenesis (23, 24). Perinatal death of IKKα$^{-/-}$ mice, however, has hampered a detailed analysis of the in vivo immunological function of IKKα. Given that NIK$^{aly/aly}$ mice have disorganized thymic structure together with an organ-specific autoimmune disease, we hypothesized that IKKα in the thymic stroma has similar roles to those of NIK. In the present study, we have examined this hypothesis and demonstrated that IKKα regulates thymic organogenesis and establishes self-tolerance primarily through a noncanonical NF-κB activation pathway with NIK, which requires the processing of NF-κB2 (i.e., production of p52 from its precursor p100) (25). With the use of isolated thymic epithelial cells (TECs) together with mTEC lines established from NIK$^{aly/aly}$ mice, we have also demonstrated that the NIK-IKKα axis regulates thymic expression of TSAs predominantly through the developmental process of mTECs, not through transcriptional control of TSA genes within developed mTECs. Thus, our results illustrate a novel function of IKKα in thymic stroma-dependent self-tolerance that cannot be compensated for by the related IKKβ subunit.

Materials and Methods

Mice

BALB/cA Jcl-*nu* mice (BALB/c$^{nu/nu}$ mice) and NIK$^{aly/aly}$ mice were purchased from CLEA Japan, and Rag2-deficient mice on BALB/c background were acquired from Taconic Farms. IKKα$^{-/-}$ mice were generated by gene targeting, as described previously (18). The mice were maintained under pathogen-free conditions and were handled in accordance with the Guidelines for Animal Experimentation of Tokushima University School of Medicine.

Thymus grafting

Thymus grafting was performed, as previously described (10). Briefly, thymic lobes were isolated from embryos at 14.5 days postcoitus and were cultured for 4 days on top of Nucleopore filters (Whatman) placed on RPMI 1640 medium (Invitrogen Life Technologies) supplemented with 10% heat-inactivated FBS (Invitrogen Life Technologies), 2 mM L-glutamine, 100 U/ml penicillin, 100 μg/ml streptomycin, 50 μM 2-ME, and 1.35 mM 2′-deoxyguanosine (2-DG; Sigma-Aldrich). Five pieces of thymic lobes were grafted under the renal capsule of BALB/c$^{nu/nu}$ mice. After 6–8 wk, reconstitution of peripheral T cells was determined by flow cytometric analysis (BD Biosciences) with anti-CD4 (clone GK1.5; BD Pharmingen) and anti-CD8 (clone 53-6.7; BD Pharmingen) mAbs, and then thymic chimeras were used for the analyses.

Western blotting

Proteins extracted from embryonic thymic lobes, prepared as described above, were analyzed with an ECL Western blotting detection system (Amersham Biosciences). Rabbit anti-peptide Abs directed against p52 (catalog no. sc-298) and RelB (catalog no. sc-226), mouse anti-*lck* mAb (catalog no. sc-433), and goat anti-actin Ab (catalog no. sc-1616) were all purchased from Santa Cruz Biotechnology.

Pathology

Formalin-fixed tissue sections were subjected to H&E staining, and two pathologists independently evaluated the histology without being informed of the detailed condition of the individual mouse. Histological changes were scored as 0 (no change), 1 (mild lymphoid cell infiltration), or 2 (marked lymphoid cell infiltration).

Establishment of TEC lines from NIK$^{aly/aly}$ mice

TEC lines were established from NIK$^{aly/aly}$ embryos at 14.5 days postcoitus, as previously described (26). These cells were maintained with gamma ray-irradiated (40 Gy) Swiss 3T3 cells as feeder cells in calcium-free MEM (Invitrogen Life Technologies) supplemented with 10% heat-inactivated FBS, 3 mM L-glutamine, 50 μg/ml gentamicin, 50 μM 2-ME, and 1 μg/ml hydrocortisone (Sigma-Aldrich). NIK$^{aly/aly}$ mouse origin was confirmed by sequencing of the *aly*-type NIK gene (6, 7).

Immunohistochemistry

Immunohistochemical analysis of the grafted thymus was performed, as previously described (10). Briefly, frozen tissue sections were fixed in cold acetone and stained by first incubating them with ER-TR5 (27) and UEA-1-biotin (Vector Laboratories). After being washed, the sections were further incubated with Alexa 594-conjugated goat anti-rat IgG (Invitrogen Life Technologies) and Alexa 488-conjugated streptavidin (Invitrogen Life Technologies) for the immunofluorescence. For the detection of autoantibodies, serum from thymic chimeras was incubated with various organs obtained from Rag2-deficient mice. FITC-conjugated anti-mouse IgG Ab (Southern Biotechnology Associates) was used for the detection. Polyclonal anti-Aire Ab was produced by immunizing rabbits with peptides corresponding to the COOH-terminal portion of mouse Aire, and Alexa 488-conjugated donkey anti-rabbit IgG (Invitrogen Life Technologies) was used as a secondary Ab for detection. TEC lines established from NIK$^{aly/aly}$ embryos were seeded on coverslips and subjected to immunohistochemistry, as previously described (28). Anti-epithelial cell adhesion molecule (Ep-CAM) mAb (BD Biosciences) and anti-keratin-5 polyclonal Ab (Covance) were used for the staining. DNA staining was with 4′6-diamidino-2-phenylindole (Roche Applied Science).

NF-κB2 processing

TECs were stimulated with agonistic anti-LTβR mAb (clone AF.H6; provided by P. Rennert, Biogen Idec) (29) (5 μg/ml) or with agonistic anti-CD40 mAb (clone 3/23; Serotec) (5 μg/ml) for 8 h. Cytoplasmic and nuclear extracts were prepared from the cells, as described previously (30), and were subjected to Western blotting with rabbit anti-p52 Ab from Upstate Biotechnology (catalogue 06-413).

Thymic stroma preparation

Thymic stroma was prepared, as described previously (17). Briefly, thymic lobes were isolated from three to six mice for each group and cut into small pieces. The fragments were gently rotated in RPMI 1640 medium (Invitrogen Life Technologies) supplemented with 10% heat-inactivated FCS (Invitrogen Life Technologies), 20 mM HEPES, 100 U/ml penicillin, 100 μg/ml streptomycin, and 50 μM 2-ME, hereafter referred to as R10, at 4°C for 30 min, and dispersed further with pipetting to remove the majority of thymocytes. The resulting thymic fragments were digested with 0.15 mg/ml collagenase IV (Sigma-Aldrich) and 10 U/ml DNase I (Roche Molecular Biochemicals) in RPMI 1640 at 37°C for 15 min. The supernatants that contained dissociated TECs were saved, whereas the remaining thymic fragments were further digested with collagenase IV and DNase I. This step was repeated twice, and the remaining thymic fragments were digested with collagenase IV, DNase I, and 0.1 mg/ml dispase I (Roche Applied Science) at 37°C for 30 min. The supernatants from this digest were combined with the supernatants from the collagenase digests, and the mixture was centrifuged for 5 min at 450 × *g*. The cells were suspended in PBS containing 5 mM EDTA and 0.5% FCS and kept on ice for 10 min. CD45$^-$ thymic stromal cells were then purified by depleting CD45$^+$ cells with MACS CD45 microbeads (Miltenyi Biotec), according to the manufacturer's instructions. The resulting preparations contained ~60% Ep-CAM$^+$ cells and <10% thymocytes (i.e., CD4/CD8 single-positive and CD4/CD8 double-positive cells), as determined by flow cytometric analysis.

Real-time PCR and semiquantitative RT-PCR

Real-time PCR for quantification of TSA genes was conducted with cDNA prepared from RNAs extracted from whole thymus or from isolated TECs. The primers, the probes, and the reactions were those described previously (10, 17). Cathepsin S primers were 5′-GCCATTCCTCCTTCTTCTTC TACA-3′ and 5′-CAAGAACACCATGATTCACATTGC-3′, and the cathepsin S probe was 5′-FAM-AAGCGGTGTCTATGATGACCCCTCCT GTA-3′ (31). Semiquantitative RT-PCR of TSA genes was conducted, as previously described (10, 17).

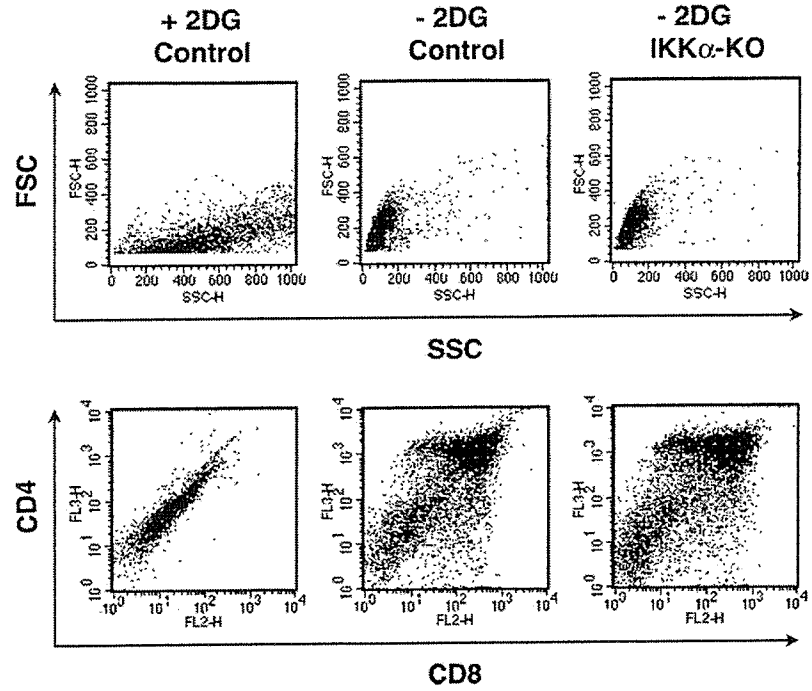

FIGURE 1. Unaltered thymocyte development in the absence of IKKα in fetal thymic organ culture. Thymic lobes isolated from embryos of both control (*center panels*) and IKK$\alpha^{-/-}$ (*right panels*) mice at 14.5 days postcoitus supported maturation of thymocytes similarly in a 4-day organ culture in the absence of 2-DG. Flow cytometric analysis with forward scatter (FSC) and side scatter (SSC) (*top panels*), and with anti-CD4 and anti-CD8 mAbs (*bottom panels*). Thymic organ culture of control mice in the presence of 2-DG is shown as a negative control (*left panels*). One representative result from a total of two repeats is shown.

Results

IKKα in the thymic stroma is required for self-tolerance

We have demonstrated recently that *aly* mice, a natural strain with mutant NIK, manifest autoimmunity resulting from disorganized thymic structure with abnormal expression of Rel proteins in the thymic stroma (10). Although the identity of the upstream receptor(s) controlling NIK-dependent thymic organogenesis has not been fully determined (see *Discussion*), we speculated that IKKα might function as a downstream kinase of NIK in this process. Because of the perinatal death of IKK$\alpha^{-/-}$ mice (18, 19), we assessed thymic organogenesis and T cell development in IKK$\alpha^{-/-}$ mice by using embryonic thymus; thymic lobes were isolated from control and IKK$\alpha^{-/-}$ embryos at 14.5 days postcoitus and cultured for 4 days in vitro. Such thymic lobes supported maturation of thymocytes similarly in both control and IKK$\alpha^{-/-}$ mice (Fig. 1), indicating a dispensable role of IKKα in both thymocytes and thymic stroma in their developmental cross talk. The dispensability of IKKα in thymocyte development assessed with this fetal thymus organ culture system is consistent with the observation of normal T cell development in chimeras in which IKK$\alpha^{-/-}$ fetal liver cells were transferred into irradiated Rag2-deficient mice (21). Of importance, histological examination of those chimeras showed no signs of autoimmune disease (T. Kaisho, K. Izumi, and M. Matsumoto, unpublished observation), suggesting that IKKα-deficient T cells do not promote the development of autoimmune disease in a cell-autonomous manner. In contrast, we speculated that IKKα in thymic stroma might be essential for the establishment of self-tolerance, as demonstrated for NIK (10). To test this hypothesis, we generated thymic chimeras. The 2-DG-treated embryonic thymic lobes, which did not contain any live thymocytes as determined by flow cytometric analysis (see Fig. 1, *left panels*) and by Western blotting with anti-*lck* Ab (see Fig. 2, *top panel*), were prepared and then grafted under the renal capsule of BALB/c$^{nu/nu}$ mice. In this system, mature T cells derived from IKKα-sufficient recipient BALB/c$^{nu/nu}$ mouse bone marrow are produced de novo through interaction with the grafted thymic stroma. Grafting both control and IKK$\alpha^{-/-}$ embryonic thymus induced T cell maturation in the periphery of BALB/c$^{nu/nu}$ mice to a similar extent: CD4$^+$ T cells plus CD8$^+$ T cells were 14.1 $\pm$ 5.3% in BALB/c$^{nu/nu}$ mice grafted with control thymus (n = 6) compared with 15.1 $\pm$ 7.6% in BALB/c$^{nu/nu}$ mice grafted with IKK$\alpha^{-/-}$ thymus (n = 7). Remarkably, histological examination of IKK$\alpha^{-/-}$ thymus-grafted mice, but not control thymus-grafted mice, revealed many lymphoid cell infiltrations in the liver, mainly in the portal area (Fig. 3, *A* and *B*), which is reminiscent of the autoimmune disease phenotype observed in NIK$^{aly/aly}$ mice. To see whether T cells developed in a thymic microenvironment without IKKα in those mice are autoreactive per se, we injected splenocytes obtained from BALB/

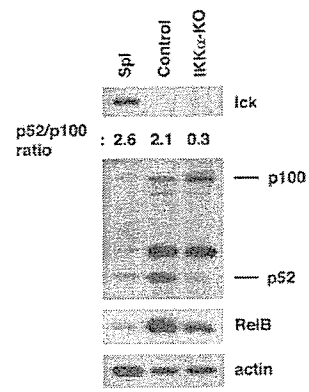

FIGURE 2. IKKα regulates the processing of NF-κB2 in thymic stroma. Thymic lobes isolated from control (*second lane*) and IKK$\alpha^{-/-}$ embryos (*third lane*), and cultured for 4 days in the presence of 2-DG contain no live thymocytes, as demonstrated by the lack of *lck* expression with Western blotting (*top panel*). The same blot was probed with anti-Rel protein Abs (*two middle panels*) and anti-actin Ab (*bottom panel*). p52 processing from the precursor p100 was impaired in thymic stroma from IKK$\alpha^{-/-}$ mice. RelB expression was also reduced in IKK$\alpha^{-/-}$ thymus. Total splenocytes (Spl) from wild-type mice were used as control (*first lane*). Intensities of the bands of p100 and p52 in each lane were measured with ImageJ software (National Institutes of Health), and the ratios between p52 and p100 are shown above the NF-κB2 Western blot. One representative result from a total of three repeats is shown.

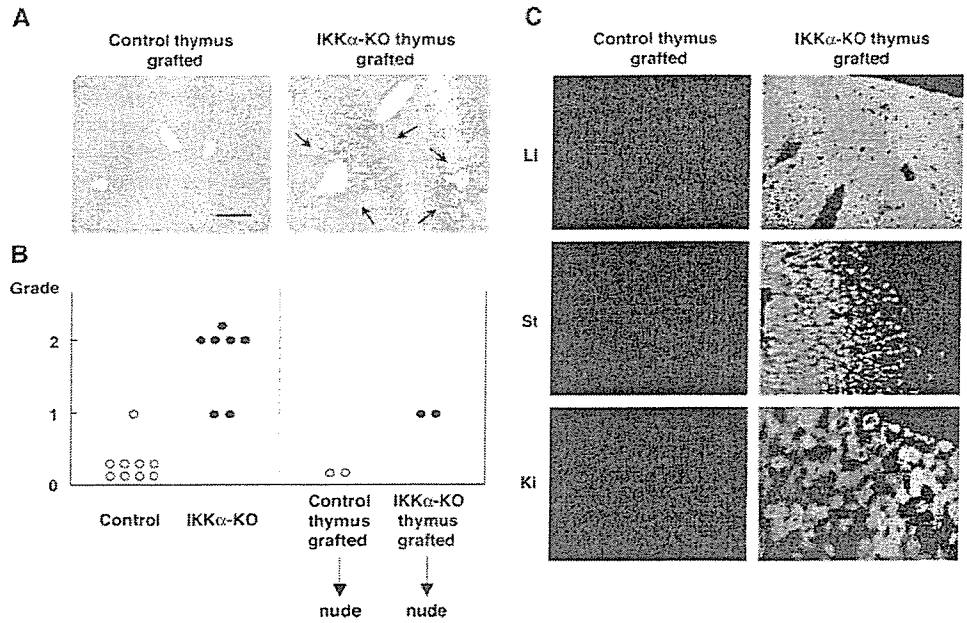

FIGURE 3. Requirement for IKKα in thymic stroma for the establishment of self-tolerance. *A*, BALB/c$^{nu/nu}$ mice grafted with IKKα$^{-/-}$ embryonic thymus (*right panel*), but not with control embryonic thymus (*left panel*), developed an autoimmune disease phenotype in the liver. Arrows indicate the lymphoid cell infiltrations. The scale bar corresponds to 100 μm in size. *B*, Many IKKα$^{-/-}$ thymus-grafted BALB/c$^{nu/nu}$ mice exhibited lymphoid cell infiltrations in the liver (●; *left half panel*). In contrast, these changes were scarcely observed in control thymus-grafted mice (○). Injection of splenocytes obtained from BALB/c$^{nu/nu}$ mice grafted with IKKα-deficient thymus into another group of BALB/c$^{nu/nu}$ mice induced lymphoid cell infiltration in the liver of the recipient mice (●; *right half panel*), whereas injection of splenocytes obtained from BALB/c$^{nu/nu}$ mice grafted with control thymus induced no such changes in the recipient mice (○). Histological changes in H&E-stained tissue sections were scored as 0 (no change), 1 (mild lymphoid cell infiltration), or 2 (marked lymphoid cell infiltration). One mark corresponds to one mouse analyzed. *C*, Serum from BALB/c$^{nu/nu}$ mice grafted with IKKα$^{-/-}$ thymus (*right panels*), but not with control thymus (*left panels*), contained IgG class autoantibodies against liver (Li; *top panels*), stomach (St; *middle panels*), and kidney (Ki; *bottom panels*) detected with immunofluorescence. Original magnification, ×100.

c$^{nu/nu}$ mice grafted with IKKα-deficient thymus into another group of BALB/c$^{nu/nu}$ mice. We observed similar lymphoid cell infiltration in the liver of the recipient mice, whereas injection of splenocytes obtained from BALB/c$^{nu/nu}$ mice grafted with control thymus induced no such changes in the recipients (Fig. 3*B*). These results clearly indicate the significance of IKKα as a thymic stromal element required for the establishment of self-tolerance. Five of seven IKKα$^{-/-}$ thymus-grafted mice also showed lymphoid cell infiltrations in the pancreas (perivascular areas near islets), although these infiltrations were less marked than in the liver (D. Kinoshita, K. Izumi, and M. Matsumoto, unpublished observation).

Development of autoimmunity in athymic *nude* mice grafted with IKKα$^{-/-}$ thymus was further demonstrated by the production of autoantibodies against various organs. When the serum from BALB/c$^{nu/nu}$ mice grafted with IKKα$^{-/-}$ thymus was tested for reactivity against liver, six of seven showed IgG class autoantibodies as detected with immunofluorescence (Fig. 3*C*). In contrast, such activity was observed in only one of six control thymus-grafted mice, and this activity was only weak. Similarly, high incidences of autoantibodies against stomach (five of seven) and kidney (six of seven) were observed in IKKα$^{-/-}$ thymus-grafted mice, although on histological examination these organs appeared unaffected when assessed 6–8 wk after thymus graft (D. Kinoshita, K. Izumi, and M. Matsumoto, unpublished observation).

IKKα in the thymic stroma regulates Rel protein expression and thymic organogenesis

Given that IKKα plays an essential role in the thymic microenvironment that is required for the establishment of self-tolerance, we investigated the expression of Rel proteins from IKKα$^{-/-}$ thymic stroma by Western blotting. Thymic lobes used for this experiment were isolated from control and IKKα$^{-/-}$ embryos at 14.5 days postcoitus and treated with 2-DG to isolate only thymic stromal elements, as described above. Expression of p52 was significantly reduced in the thymic stroma from IKKα$^{-/-}$ mice compared with that from control mice, whereas p100, a precursor form of p52, was more abundant in IKKα$^{-/-}$ mice than in control mice (Fig. 2); the amount of p52 in thymic stroma from control mice was double that of p100, whereas the ratio of p52 to p100 was reversed in IKKα$^{-/-}$ mice. Thus, IKKα-dependent generation of p52 from p100 in thymic stroma might constitute a second NF-κB signaling pathway, as we originally observed in hemopoietic cells (32) and subsequently characterized for signals through LTβR (33), CD40 (34), and B cell activating factor of the TNF family receptor (35, 36). RelB expression in the thymic stroma was slightly reduced in IKKα$^{-/-}$ mice compared with that in control mice (Fig. 2), as observed in NIK$^{aly/aly}$ mice (10). These results suggest that the disturbed thymic microenvironment in IKKα$^{-/-}$ mice is associated with abnormal regulation of the NF-κB activation pathway in the thymic stroma in the absence of IKKα.

The essential roles of IKKα in thymic stroma were also confirmed by histological examination of the grafted thymus. Although embryonic thymus from control mice that had been grafted onto BALB/c$^{nu/nu}$ mice contained mTECs that bound with UEA-1, IKKα$^{-/-}$ embryonic thymus grafted onto BALB/c$^{nu/nu}$ mice did not have UEA-1^{+} cells (Fig. 4*A*). ER-TR5^{+} mTECs were sparse in IKKα$^{-/-}$ embryonic thymus grafted onto BALB/c$^{nu/nu}$ mice compared with control embryonic thymus grafted similarly (Fig. 4*A*). Abnormal development of mTECs in the absence of IKKα

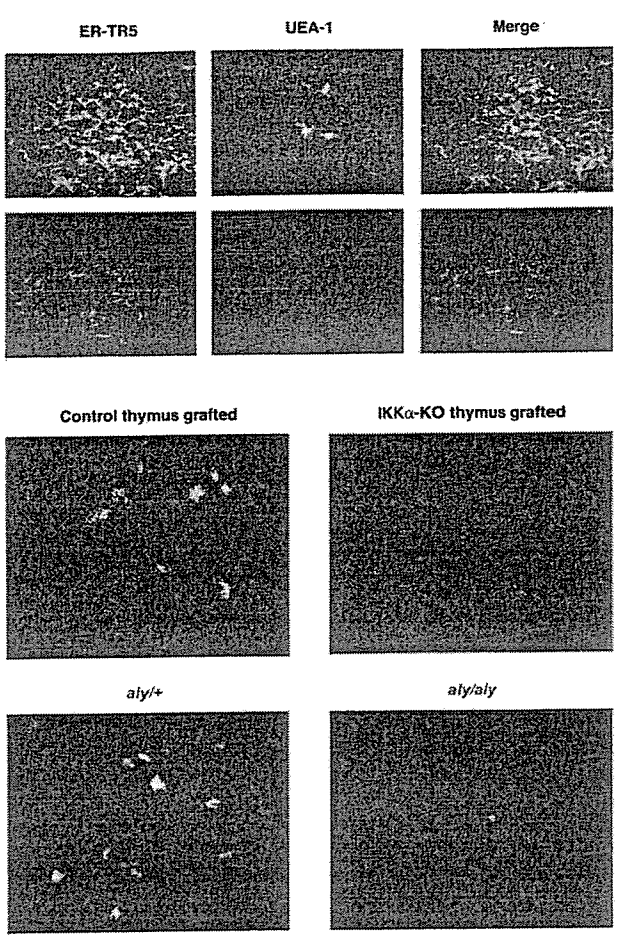

FIGURE 4. IKKα is required for thymic organization. *A*, Embryonic thymus from IKK$\alpha^{-/-}$ mice contained no UEA-1$^+$ cells (*bottom middle panel*) and fewer ER-TR5$^+$ medullary epithelial cells stained in red (*bottom left panel*) after grafting onto BALB/c$^{nu/nu}$ mice compared with that from control mice (*top left panel*). UEA-1$^+$ cells from control embryonic thymus grafted onto BALB/c$^{nu/nu}$ mice were stained in green (*top middle panel*), and were merged with ER-TR5 staining (*top right panel*). *B*, Embryonic thymus from IKK$\alpha^{-/-}$ mice grafted onto BALB/c$^{nu/nu}$ mice contained very few Aire$^+$ cells (*top right panel*), as observed in adult untreated NIK$^{aly/aly}$ thymus (*bottom right panel*). Aire$^+$ cells were observed in embryonic thymus from control mice grafted onto BALB/c$^{nu/nu}$ mice (*top left panel*) and adult untreated NI-K$^{aly/+}$ thymus (*bottom left panel*). Original magnification, ×200. One representative result from a total of five repeats is shown.

was also exemplified by the loss of Aire$^+$ cells in IKK$\alpha^{-/-}$ embryonic thymus grafted onto BALB/c$^{nu/nu}$ mice (Fig. 4*B*). A dramatic decrease in the number of Aire$^+$ cells was also observed in adult untreated NIK$^{aly/aly}$ thymus (Fig. 4*B*). Because T cells with normal IKKα (derived from BALB/c$^{nu/nu}$ mice) cannot restore normal mTECs in the IKK$\alpha^{-/-}$ thymus when the interaction between T cells and thymic stromal cells is initiated from the embryonic stage, the contribution of IKKα to thymic organogenesis seems to be stromal element autonomous. These results clearly indicate indispensable roles for IKKα as a stromal element in the thymic organogenesis that is required for the establishment of self-tolerance.

Developmental effect of NIK for promiscuous gene expression in the thymus

Promiscuous gene expression of many TSAs in mTECs could play an essential role in the establishment of central tolerance (12). The autoimmunity developed in NIK$^{aly/aly}$ mice (10) and IKK$\alpha^{-/-}$ mice, described above, might be associated with altered expression of self Ags in the thymus. In fact, NIK$^{aly/aly}$ thymus showed dramatically reduced transcription of many TSAs (10). We have examined whether thymic expression of TSAs is influenced by the absence of IKKα using embryonic thymus grafted onto BALB/c$^{nu/nu}$ mice; RNAs were extracted from the thymus 6 wk after grafting when the thymus was colonized with developing thymocytes derived from BALB/c$^{nu/nu}$ mouse bone marrow. By real-time PCR, salivary protein 1 (SP1), fatty acid-binding protein (FABP), C-reactive protein (CRP), and glutamic acid decarboxylase 67 (GAD67) were easily detected in grafted control thymus, whereas expression of SP1, FABP, and GAD67 was below the limit of detection in grafted IKK$\alpha^{-/-}$ thymus. Although CRP was detected in grafted IKK$\alpha^{-/-}$ thymus (N. Kuroda and M. Matsumoto, unpublished observation), its expression was reduced; the value for *CRP/hypoxanthine phosphoribosyltransferase* (*HPRT*) from control thymus was 1.61, and that for *CRP/HPRT* from IKK$\alpha^{-/-}$ thymus was 0.32.

Because we used RNAs extracted from total thymus instead of isolated mTECs in both previous experiments with NIK$^{aly/aly}$ mice (10) and experiments with IKK$\alpha^{-/-}$ thymic chimeras described above, it is not clear whether reduced expression of TSAs was due to the reduced number of mTECs expressing TSAs (15) or to the lack of NIK-IKKα-dependent transcriptional control of TSA genes. To test these possibilities, we harvested TECs (which contain both cortical and medullary components) from adult NI-K$^{aly/aly}$ mice and examined the expression of TSAs together with cathepsin S (CAT-S), which is highly expressed by mTECs in the thymic stroma (31). Consistent with immunohistochemical evaluation demonstrating less abundant mTECs in NIK$^{aly/aly}$ mice (10), TECs purified from NIK$^{aly/aly}$ thymus showed reduced expression of CAT-S (Table I): the ratio between the values from NIK$^{aly/+}$ mice and NIK$^{aly/aly}$ mice was 0.12. When RNAs extracted from purified TECs were tested for TSA expression by real-time PCR using HPRT as an internal control, the difference between NI-K$^{aly/+}$ and NIK$^{aly/aly}$ mice became subtle when compared with the results obtained from total thymus, except for CRP (Table I). This

Table I. *Expression of tissue-specific genes in the thymus*[a]

Genotype	SP1	FABP	CRP	GAD67	CAT-S
aly/+	7.97/6.28	6.10/7.62	1.30/3.04	7.18/3.80	N.A./12.2[b]
aly/aly	7.45×10^{-2}/18.2	4.08×10^{-2}/0.21	9.49×10^{-2}/0.14	4.44×10^{-2}/0.64	N.A./1.44
Relative abundance[c] (*aly/aly* vs *aly/+*)	0.93×10^{-2}/2.90	0.67×10^{-2}/0.03	0.07/0.05	0.62×10^{-2}/0.17	N.A./0.12

[a] Real-time PCR for peripheral tissue-specific genes (i.e., *SP1, FABP, CRP, GAD67,* and *CAT-S*) was performed using RNAs extracted from total thymus (shown on the left) or RNAs extracted from purified TECs (shown on the right) from NIK$^{aly/+}$ and NIK$^{aly/aly}$ mice. *Hprt* expression level was used as an internal control. Pools of TECs isolated from three to six mice of each group were used for the analysis. One representative result from a total of two repeats is shown.

[b] N.A., Not applicable.

[c] The relative abundance of each gene was calculated from the ratio between the values from NIK$^{aly/+}$ mice and NIK$^{aly/aly}$ mice (e.g., the *SP1/Hprt* value from NIK$^{aly/aly}$ mice was divided by the *SP1/Hprt* value from NIK$^{aly/+}$ mice).

finding is more obvious when taking into account that TECs purified from NIK$^{aly/aly}$ thymus contained reduced mTEC components compared with those from NIK$^{aly/+}$ thymus, as revealed by the reduced expression of CAT-S. These results suggest that NIK regulates thymic expression of TSAs predominantly through the developmental process of mTECs, and not through transcriptional control of TSA genes within developed mTECs.

To further confirm this finding, we used mTEC lines established from the thymus. Because we were not able to establish TEC lines from IKK$\alpha^{-/-}$ embryos at 18.5 days postcoitus for unknown reasons, we used mTEC lines established from NIK$^{aly/aly}$ embryos for this purpose; it is possible that the protein kinase-independent function of IKKα may contribute to the growth disadvantage of TECs lacking IKKα (23, 24). We established three cell lines from NIK$^{aly/aly}$ embryonic thymus (5-1, 4-1-3, and 6-5T), and these cells were positive for Ep-CAM, an epithelial cell marker, and staining with keratin-5 and ER-TR5 (Fig. 5*A*), but negative for keratin-8 and Th-3 (Ref. 26 and Y. Mouri, M. Kasai, and M. Matsumoto, unpublished observation), consistent with a medullary origin. The TEC origin of these lines was also verified by Foxn1 expression (Fig. 5*C*). In these NIK$^{aly/aly}$ mTECs, agonistic stimulation of LTβR by mAb AF.H6 (29) did not induce NF-κB2 processing, in contrast to the mTECs derived from wild-type C57BL/6 mice (26) (Fig. 5*B*); LTβR ligation on wild-type mTEC increased amount of p52 in the nucleus (Nucl; *bottom panel*) with a concomitant reduction of p100 in the cytoplasm (Cyto; *top panel*), whereas the same treatment induced no nuclear p52 in NIK$^{aly/aly}$ mTEC. In contrast, CD40 ligation on both wild-type and NIK$^{aly/aly}$ mTECs had no such effect, which is consistent with the fact that CD40$^{-/-}$ mice showed undisturbed thymic architecture with normal distribution of mTECs containing UEA-1^{+} cells, ER-TR5^{+} cells, and Aire^{+} cells (Y. Mouri and M. Matsumoto, unpublished observation). Thus, these established cell lines show many of the characteristics of mTECs while retaining the features of *aly*-type NIK mutation.

mTEC lines established from NIK$^{aly/aly}$ mice showed levels of TSAs that were indistinguishable from those of control mTECs (Fig. 5*C*): SP1 and FABP were expressed from all the lines from both wild-type and NIK$^{aly/aly}$ mTECs. Expression of CRP assessed with real-time PCR was also indistinguishable between wild-type and NIK$^{aly/aly}$ mTECs: *CRP/HPRT* values from wild-type mTECs were 4.93 (line 2-3), 1.04 (line 1C6), and 2.21 (line 3-10), and *CRP/HPRT* values from NIK$^{aly/aly}$ mTECs were 2.75 (line 5-1), 1.67 (line 4-1-3), and 3.01 (line 6-5T). Insulin/*HPRT* values from wild-type mTECs were 0.47 (line 1C6) and 1.66 (line 3-10), and insulin/*HPRT* values from NIK$^{aly/aly}$ mTECs were 0.50 (line 5-1), 0.33 (line 4-1-3), and 0.65 (line 6-5T). Taken together, these results suggest that NIK is not required in individual mTECs for the transcriptional control of TSA genes. Rather, reduced expression of TSAs in NIK$^{aly/aly}$ thymus is most likely due to the developmental effect of mutated NIK on mTECs, leading to reduced absolute numbers of mTECs, each expressing normal levels of TSAs.

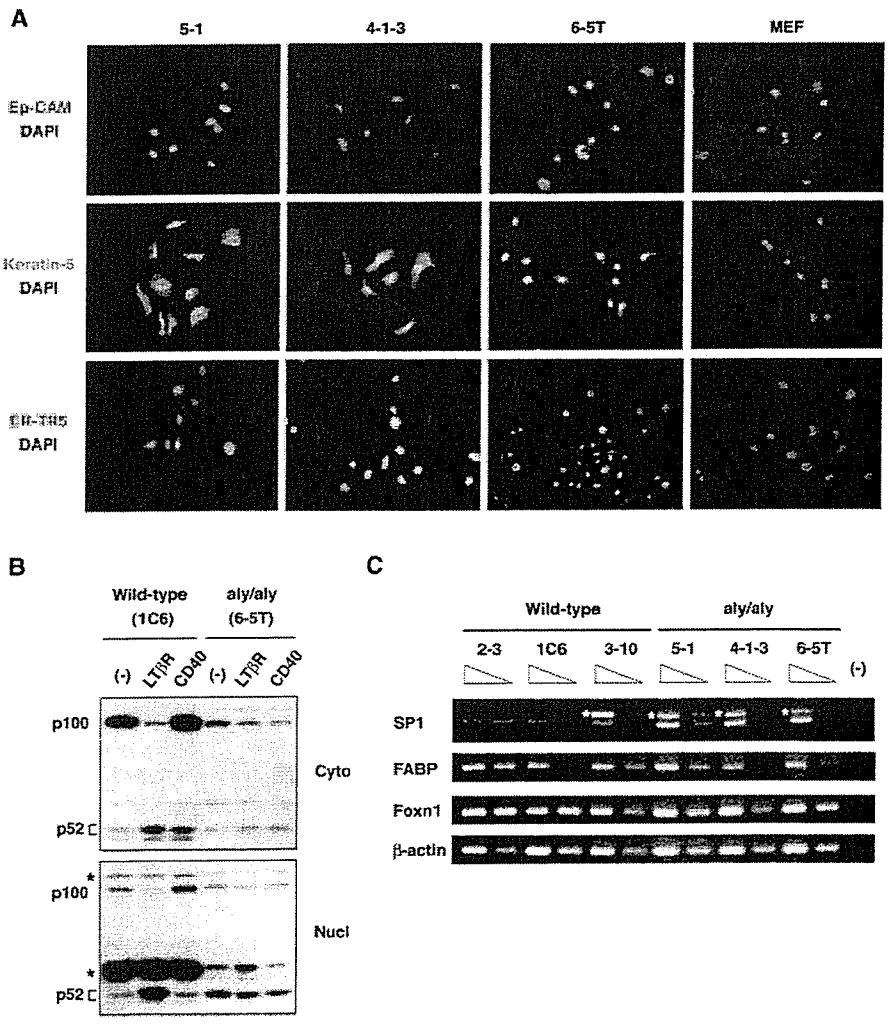

FIGURE 5. Retained expression of TSA genes in mTEC lines established from NIK$^{aly/aly}$ thymus. *A*, TEC lines established from NIK$^{aly/aly}$ embryos (5-1, 4-1-3, and 6-5T) were positive for Ep-CAM (*top panels*, stained in red), keratin-5 (*middle panels*, stained in green), and ER-TR5 (*bottom panels*, stained in red). Mouse embryonic fibroblasts (MEF) served as negative control. DNA staining is with 4′6-diamidino-2-phenylindole (stained in blue). Original magnification, ×200. *B*, In wild-type mTEC (1C6), but not in NIK$^{aly/aly}$ mTEC (6-5T), LTβR ligation with agonistic anti-LTβR mAb increased amount of nuclear p52 (Nucl; *bottom panel*) with a concomitant reduction of p100 in the cytoplasm (Cyto; *top panel*). Such effect was observed in neither wild-type nor NIK$^{aly/aly}$ mTECs upon CD40 stimulation. One representative result from a total of three repeats is shown. Asterisks denote nonspecific bands. *C*, Semiquantitative RT-PCR for peripheral tissue-specific genes (SP1; FABP) was performed using mTECs established from control and NIK$^{aly/aly}$ thymus. The TEC origin of these cell lines was verified by Foxn1 expression. β-actin was used to verify equal amounts of RNAs in each sample. One representative result from a total of three repeats is shown. Asterisks denote nonspecific bands. −, Without template.

Based on the similarity of autoimmune phenotypes between NIK$^{aly/aly}$ thymus and IKK$\alpha^{-/-}$ thymus, we speculate that IKKα regulates TSA expression in the thymus through a developmental effect similar to that of NIK.

Discussion

We have demonstrated that IKKα plays an essential role in the organization of the thymic microenvironment that is required for the establishment of central tolerance. Grafting the thymic stroma from IKK$\alpha^{-/-}$ mice onto athymic *nude* mice led to the development of autoimmune disease in the recipients; this also occurred in another group of recipient mice when the splenocytes from the IKK$\alpha^{-/-}$ thymus-grafted mice were transferred. The thymic microenvironment that caused autoimmune disease in an IKKα-dependent manner was associated with structural abnormality (lack of UEA-1$^+$ cells, and sparse ER-TR5$^+$ and Aire$^+$ cells in the medulla), defective NF-κB2 activation (impaired processing of p100 into p52), and reduced expression of TSAs. Because those phenotypes were similarly observed in NIK$^{aly/aly}$ mice (10), it is reasonable to speculate that the NIK-IKKα axis constitutes an essential step in this action, as demonstrated for secondary lymphoid organogenesis through LTβR involving NF-κB2 processing (7, 20, 37).

We have suggested that impaired processing of p100 into p52 caused by mutated NIK (10) or a lack of IKKα, as demonstrated in the present study, is relevant to the developmental defect of the thymic microenvironment. This reasoning is apparently inconsistent with the fact that mice deficient for p52 show no major defect in the thymus (38, 39). We interpret this discrepancy as a dominant effect of p100 on NF-κB activation in thymic stroma; accumulation of p100, rather than absence of p52, might be responsible for the thymic phenotypes we observed. In fact, mice lacking the COOH-terminal ankyrin domain of NF-κB2 (i.e., p100), but still containing a functional p52 protein, show abnormal development of the thymus (40), indicating the relevance of p100 to the control of thymic organogenesis. Notably, the mice deficient for p52 described above lack the whole NF-κB2 protein (including p100) because of the targeted deletion of the NF-κB2 gene locus (38, 39). We therefore consider that the ratio between p100 and p52 is a critical determinant for proper activation of the NF-κB complex that contains RelB as a heterodimeric partner (see below). Accumulation of p100 could disturb the nuclear localization of activated NF-κB complex within mTECs.

Although the exact mechanism by which IKKα regulates the thymic microenvironment that is required for the establishment of central tolerance is unknown, the existence of disorganized thymic structure together with an autoimmune disease phenotype in mice with a mutation disrupting the RelB gene merits attention. Because of the phenotypic similarities between NIK mutant mice and RelB$^{-/-}$ mice (41) (multi-inflammatory lesions together with the absence of UEA-1$^+$ mTECs), together with the roles of IKKα demonstrated in the present study, we speculate that NIK-IKKα regulates the thymic microenvironment through activation of the NF-κB complex containing RelB. A requirement for NIK for activation of the NF-κB complex containing RelB is also seen in the production of NK T cells (41, 42). Interestingly, TNFR-associated factor 6 (TRAF6) in TECs is a critical component that regulates RelB expression, thereby controlling the thymic microenvironment for the establishment of central tolerance (43). Although both NIK-IKKα-dependent and TRAF6-dependent signals merge at the level of the NF-κB complex (i.e., p52/RelB), it is reasonable to speculate that the upstream receptors of each signal are distinct, because many NIK-IKKα-dependent signals are TRAF6 independent, as exemplified for LTβR (43), and vice versa. These results suggest the existence of a group of receptor-mediated signals that together control thymic organogenesis. The mechanisms that control the specificity of the heterodimeric complex of Rel family members (e.g., p52/RelB or p50/RelA) according to cell type and/or cellular signals also need to be clarified by future studies.

Signaling through LTβR has been demonstrated recently to control thymic organogenesis (44). However, because NIK$^{aly/aly}$ mice show more severe phenotypes of thymic structure than do LTβR-deficient mice (44), it would be reasonable to speculate that the NIK-IKKα axis is acting downstream of additional receptor(s) beyond LTβR in thymic organogenesis. Because CD40 is expressed on TECs (45, 46), and NF-κB2 processing takes place downstream of CD40, at least in B cells (34), CD40 could be a good candidate for an additional receptor that acts in NIK-IKKα-dependent thymic organogenesis. However, CD40$^{-/-}$ mice showed undisturbed thymic architecture with normal distribution of mTECs containing UEA-1$^+$ cells, ER-TR5$^+$ cells, and Aire$^+$ cells (Y. Mouri and M. Matsumoto, unpublished observation), suggesting that CD40 alone is not responsible for this action. Consistent with this finding, CD40 ligation on wild-type mTEC (and NIK$^{aly/aly}$ mTEC as well) induced no NF-κB2 processing (Fig. 5*B*), although flow cytometric analysis clearly demonstrated CD40 expression on both mTEC lines (S. Niki and M. Matsumoto, unpublished observation). A complete description of the upstream receptor(s) required for thymic organogenesis in a NIK-IKKα-dependent manner is essential for a better understanding of the roles of NF-κB in the establishment of central tolerance.

The cellular mechanism controlling the establishment of self-tolerance in an IKKα-dependent manner is of considerable interest. Because of the perinatal death of IKK$\alpha^{-/-}$ mice, we have investigated most of the IKKα-dependent autoimmune disease process with thymic chimeras. Because the autoimmune disease phenotype in NIK$^{aly/aly}$ mice is a result of both impaired elimination of autoreactive T cells and impaired production of Tregs (10), we suggest similar mechanisms for the breakdown of self-tolerance in the thymic microenvironment lacking IKKα. Consistent with this hypothesis, when control thymus and IKK$\alpha^{-/-}$ thymus were grafted simultaneously onto BALB/c$^{nu/nu}$ mice, the development of inflammatory lesions was not completely inhibited (D. Kinoshita, K. Izumi, and M. Matsumoto, unpublished observation), suggesting that the grafted IKK$\alpha^{-/-}$ thymus allows production of more pathogenic autoreactive T cells in the recipient mice than can be controlled by the Tregs that are produced by the grafted control thymus. We speculate that thymic stroma that has developed in the absence of IKKα may not be able to present TCR ligands (most likely containing self peptides) efficiently enough, resulting in insufficient avidity for the elimination of autoreactive T cells and/or production of Tregs (13, 14).

The autoimmunity that developed in NIK$^{aly/aly}$ mice (10) and IKK$\alpha^{-/-}$ mice, described in the present study, was associated with altered expression of self Ags in the thymus, although the significance of this finding requires further study. We investigated whether reduced expression of self Ags in a NIK-IKKα-dependent manner was due to a reduction in the number of mTECs expressing these Ags or a lack of TSA gene transcription in these cells. Because purified TECs from NIK$^{aly/aly}$ thymus largely restored TSA expression, and the levels of TSAs expressed by mTEC lines isolated from NIK$^{aly/aly}$ mice were indistinguishable from the levels expressed by wild-type mTEC lines, the reduced TSA expression by total NIK$^{aly/aly}$ thymus is most likely due to the effect of the NIK-IKKα axis on the development of mTECs. Consistent with this finding, sorted TECs from LTβR-deficient mice (which have thymic disorganization and absolute reduction of TEC number) demonstrated unaltered expression of TSA genes (44). In contrast, Aire affects TSA expression without any obvious structural abnormalities of the thymus (16, 17). Thus, TSA expression in mTECs

is controlled by a group of genes through their unique actions. Identification of particular cell types responsible for TSA expression, together with the nature of the TCR ligands (possibly TSA gene products) required for the establishment of self-tolerance, awaits further study. With the advent of thymic organogenesis using thymic precursor cells (47, 48), it may be feasible to manipulate the thymic microenvironment through the modulation of NF-κB activation pathways, thereby controlling the processes for the establishment of self-tolerance.

Acknowledgments

We thank Drs. W. van Ewijk and M. Itoi for mAb ER-TR5, and Dr. P. D. Rennert for mAb AF.H6. We also thank Drs. H. Nakano and J. Inoue for valuable suggestions.

Disclosures

The authors have no financial conflict of interest.

References

1. Li, Q., and I. M. Verma. 2002. NF-κB regulation in the immune system. *Nat. Rev. Immunol.* 2: 725–734.
2. Karin, M., and A. Lin. 2002. NF-κB at the crossroads of life and death. *Nat. Immunol.* 3: 221–227.
3. Ling, L., Z. Cao, and D. V. Goeddel. 1998. NF-κB-inducing kinase activates IKK-α by phosphorylation of Ser-176. *Proc. Natl. Acad. Sci. USA* 95: 3792–3797.
4. Malinin, N. L., M. P. Boldin, A. V. Kovalenko, and D. Wallach. 1997. MAP3K-related kinase involved in NF-κB induction by TNF, CD95 and IL-1. *Nature* 385: 540–544.
5. Miyawaki, S., Y. Nakamura, H. Suzuka, M. Koba, R. Yasumizu, S. Ikehara, and Y. Shibata. 1994. A new mutation, *aly*, that induces a generalized lack of lymph nodes accompanied by immunodeficiency in mice. *Eur. J. Immunol.* 24: 429–434.
6. Shinkura, R., K. Kitada, F. Matsuda, K. Tashiro, K. Ikuta, M. Suzuki, K. Kogishi, T. Serikawa, and T. Honjo. 1999. Alymphoplasia is caused by a point mutation in the mouse gene encoding Nf-κB-inducing kinase. *Nat. Genet.* 22: 74–77.
7. Matsushima, A., T. Kaisho, P. D. Rennert, H. Nakano, K. Kurosawa, D. Uchida, K. Takeda, S. Akira, and M. Matsumoto. 2001. Essential role of nuclear factor (NF)-κB-inducing kinase and inhibitor of κB (IκB) kinase α in NF-κB activation through lymphotoxin β receptor, but not through tumor necrosis factor receptor I. *J. Exp. Med.* 193: 631–636.
8. Matsumoto, M. 1999. Role of TNF ligand and receptor family in the lymphoid organogenesis defined by gene targeting. *J. Med. Invest.* 46: 141–150.
9. Matsumoto, M., K. Iwamasa, P. D. Rennert, T. Yamada, R. Suzuki, A. Matsushima, M. Okabe, S. Fujita, and M. Yokoyama. 1999. Involvement of distinct cellular compartments in the abnormal lymphoid organogenesis in lymphotoxin-α-deficient mice and alymphoplasia (*aly*) mice defined by the chimeric analysis. *J. Immunol.* 163: 1584–1591.
10. Kajiura, F., S. Sun, T. Nomura, K. Izumi, T. Ueno, Y. Bando, N. Kuroda, H. Han, Y. Li, A. Matsushima, et al. 2004. NF-κB-inducing kinase establishes self-tolerance in a thymic stroma-dependent manner. *J. Immunol.* 172: 2067–2075.
11. von Boehmer, H., I. Aifantis, F. Gounari, O. Azogui, L. Haughn, I. Apostolou, E. Jaeckel, F. Grassi, and L. Klein. 2003. Thymic selection revisited: how essential is it? *Immunol. Rev.* 191: 62–78.
12. Kyewski, B., and J. Derbinski. 2004. Self-representation in the thymus: an extended view. *Nat. Rev. Immunol.* 4: 688–698.
13. Shevach, E. M. 2002. CD4$^+$CD25$^+$ suppressor T cells: more questions than answers. *Nat. Rev. Immunol.* 2: 389–400.
14. Sakaguchi, S. 2004. Naturally arising CD4$^+$ regulatory T cells for immunologic self-tolerance and negative control of immune responses. *Annu. Rev. Immunol.* 22: 531–562.
15. Derbinski, J., A. Schulte, B. Kyewski, and L. Klein. 2001. Promiscuous gene expression in medullary thymic epithelial cells mirrors the peripheral self. *Nat. Immunol.* 2: 1032–1039.
16. Anderson, M. S., E. S. Venanzi, L. Klein, Z. Chen, S. Berzins, S. J. Turley, H. Von Boehmer, R. Bronson, A. Dierich, C. Benoist, and D. Mathis. 2002. Projection of an immunological self-shadow within the thymus by the Aire protein. *Science* 298: 1395–1401.
17. Kuroda, N., T. Mitani, N. Takeda, N. Ishimaru, R. Arakaki, Y. Hayashi, Y. Bando, K. Izumi, T. Takahashi, T. Nomura, et al. 2005. Development of autoimmunity against transcriptionally unrepressed target antigen in the thymus of Aire-deficient mice. *J. Immunol.* 174: 1862–1870.
18. Takeda, K., O. Takeuchi, T. Tsujimura, S. Itami, O. Adachi, T. Kawai, H. Sanjo, K. Yoshikawa, N. Terada, and S. Akira. 1999. Limb and skin abnormalities in mice lacking IKKα. *Science* 284: 313–316.
19. Hu, Y., V. Baud, M. Delhase, P. Zhang, T. Deerinck, M. Ellisman, R. Johnson, and M. Karin. 1999. Abnormal morphogenesis but intact IKK activation in mice lacking the IKKα subunit of IκB kinase. *Science* 284: 316–320.
20. Senftleben, U., Y. Cao, G. Xiao, F. R. Greten, G. Krahn, G. Bonizzi, Y. Chen, Y. Hu, A. Fong, S. C. Sun, and M. Karin. 2001. Activation by IKKα of a second, evolutionary conserved, NF-κB signaling pathway. *Science* 293: 1495–1499.
21. Kaisho, T., K. Takeda, T. Tsujimura, T. Kawai, F. Nomura, N. Terada, and S. Akira. 2001. IκB kinase α is essential for mature B cell development and function. *J. Exp. Med.* 193: 417–426.
22. Cao, Y., G. Bonizzi, T. N. Seagroves, F. R. Greten, R. Johnson, E. V. Schmidt, and M. Karin. 2001. IKKα provides an essential link between RANK signaling and cyclin D1 expression during mammary gland development. *Cell* 107: 763–775.
23. Hu, Y., V. Baud, T. Oga, K. I. Kim, K. Yoshida, and M. Karin. 2001. IKKα controls formation of the epidermis independently of NF-κB. *Nature* 410: 710–714.
24. Sil, A. K., S. Maeda, Y. Sano, D. R. Roop, and M. Karin. 2004. IκB kinase-α acts in the epidermis to control skeletal and craniofacial morphogenesis. *Nature* 428: 660–664.
25. Pomerantz, J. L., and D. Baltimore. 2002. Two pathways to NF-κB. *Mol. Cell* 10: 693–695.
26. Kasai, M., and K. Hirokawa. 1991. A novel cofactor produced by a thymic epithelial cell line: promotion of proliferation of immature thymic lymphocytes by the presence of interleukin-1 and various mitogens. *Cell. Immunol.* 132: 377–390.
27. van Vliet, E., M. Melis, and W. van Ewijk. 1984. Monoclonal antibodies to stromal cell types of the mouse thymus. *Eur. J. Immunol.* 14: 524–529.
28. Akiyoshi, H., S. Hatakeyama, J. Pitkanen, Y. Mouri, V. Doucas, J. Kudoh, K. Tsurugaya, D. Uchida, A. Matsushima, K. Oshikawa, et al. 2004. Subcellular expression of autoimmune regulator (AIRE) is organized in a spatiotemporal manner. *J. Biol. Chem.* 279: 33984–33991.
29. Rennert, P. D., D. James, F. Mackay, J. L. Browning, and P. S. Hochman. 1998. Lymph node genesis is induced by signaling through the lymphotoxin β receptor. *Immunity* 9: 71–79.
30. Matsumoto, M., T. Yamada, S. K. Yoshinaga, T. Boone, T. Horan, S. Fujita, Y. Li, and T. Mitani. 2002. Essential role of NF-κB-inducing kinase in T cell activation through the TCR/CD3 pathway. *J. Immunol.* 169: 1151–1158.
31. Gallegos, A. M., and M. J. Bevan. 2004. Central tolerance to tissue-specific antigens mediated by direct and indirect antigen presentation. *J. Exp. Med.* 200: 1039–1049.
32. Yamada, T., T. Mitani, K. Yorita, D. Uchida, A. Matsushima, K. Iwamasa, S. Fujita, and M. Matsumoto. 2000. Abnormal immune function of hemopoietic cells from alymphoplasia (*aly*) mice, a natural strain with mutant NF-κB-inducing kinase. *J. Immunol.* 165: 804–812.
33. Xiao, G., E. W. Harhaj, and S. C. Sun. 2001. NF-κB-inducing kinase regulates the processing of NF-κB2 p100. *Mol. Cell* 7: 401–409.
34. Coope, H. J., P. G. Atkinson, B. Huhse, M. Belich, J. Janzen, M. J. Holman, G. G. Klaus, L. H. Johnston, and S. C. Ley. 2002. CD40 regulates the processing of NF-κB2 p100 to p52. *EMBO J.* 21: 5375–5385.
35. Kayagaki, N., M. Yan, D. Seshasayee, H. Wang, W. Lee, D. M. French, I. S. Grewal, A. G. Cochran, N. C. Gordon, J. Yin, et al. 2002. BAFF/BLyS receptor 3 binds the B cell survival factor BAFF ligand through a discrete surface loop and promotes processing of NF-κB2. *Immunity* 17: 515–524.
36. Claudio, E., K. Brown, S. Park, H. Wang, and U. Siebenlist. 2002. BAFF-induced NEMO-independent processing of NF-κB2 in maturing B cells. *Nat. Immunol.* 3: 958–965.
37. Dejardin, E., N. M. Droin, M. Delhase, E. Haas, Y. Cao, C. Makris, Z. W. Li, M. Karin, C. F. Ware, and D. R. Green. 2002. The lymphotoxin-β receptor induces different patterns of gene expression via two NF-κB pathways. *Immunity* 17: 525–535.
38. Caamano, J. H., C. A. Rizzo, S. K. Durham, D. S. Barton, C. Raventos-Suarez, C. M. Snapper, and R. Bravo. 1998. Nuclear factor (NF)-κB2 (p100/p52) is required for normal splenic microarchitecture and B cell-mediated immune responses. *J. Exp. Med.* 187: 185–196.
39. Franzoso, G., L. Carlson, L. Poljak, E. W. Shores, S. Epstein, A. Leonardi, A. Grinberg, T. Tran, T. Scharton-Kersten, M. Anver, et al. 1998. Mice deficient in nuclear factor (NF)-κB/p52 present with defects in humoral responses, germinal center reactions, and splenic microarchitecture. *J. Exp. Med.* 187: 147–159.
40. Ishikawa, H., D. Carrasco, E. Claudio, R. P. Ryseck, and R. Bravo. 1997. Gastric hyperplasia and increased proliferative responses of lymphocytes in mice lacking the COOH-terminal ankyrin domain of NF-κB2. *J. Exp. Med.* 186: 999–1014.
41. Sivakumar, V., K. J. Hammond, N. Howells, K. Pfeffer, and F. Weih. 2003. Differential requirement for Rel/nuclear factor κB family members in natural killer T cell development. *J. Exp. Med.* 197: 1613–1621.
42. Elewaut, D., R. B. Shaikh, K. J. Hammond, H. De Winter, A. J. Leishman, S. Sidobre, O. Turovskaya, T. I. Prigozy, L. Ma, T. A. Banks, et al. 2003. NIK-dependent RelB activation defines a unique signaling pathway for the development of Vα 14i NKT cells. *J. Exp. Med.* 197: 1623–1633.
43. Akiyama, T., S. Maeda, S. Yamane, K. Ogino, M. Kasai, F. Kajiura, M. Matsumoto, and J. Inoue. 2005. Dependence of self-tolerance on TRAF6-directed development of thymic stroma. *Science* 308: 248–251.
44. Boehm, T., S. Scheu, K. Pfeffer, and C. C. Bleul. 2003. Thymic medullary epithelial cell differentiation, thymocyte emigration, and the control of autoimmunity require lympho-epithelial cross talk via LTβR. *J. Exp. Med.* 198: 757–769.
45. Galy, A. H., and H. Spits. 1992. CD40 is functionally expressed on human thymic epithelial cells. *J. Immunol.* 149: 775–782.
46. Dunn, R. J., C. J. Luedecker, H. S. Haugen, C. H. Clegg, and A. G. Farr. 1997. Thymic overexpression of CD40 ligand disrupts normal thymic epithelial organization. *J. Histochem. Cytochem.* 45: 129–141.
47. Gill, J., M. Malin, G. A. Hollander, and R. Boyd. 2002. Generation of a complete thymic microenvironment by MTS24$^+$ thymic epithelial cells. *Nat. Immunol.* 3: 635–642.
48. Bennett, A. R., A. Farley, N. F. Blair, J. Gordon, L. Sharp, and C. C. Blackburn. 2002. Identification and characterization of thymic epithelial progenitor cells. *Immunity* 16: 803–814.

IL-27 Suppresses CD28-Medicated IL-2 Production through Suppressor of Cytokine Signaling 3[1]

Toshiyuki Owaki,*† Masayuki Asakawa,*‡ Sadahiro Kamiya,§ Kiyoshi Takeda,¶ Fumio Fukai,† Junichiro Mizuguchi,*‡ and Takayuki Yoshimoto[2]*

IL-27 is a novel IL-6/IL-12 family cytokine that not only plays a role in the early regulation of Th1 differentiation, but also exerts an inhibitory effect on immune responses, including the suppression of proinflammatory cytokine production. However, the molecular mechanism by which IL-27 exerts the inhibitory effect remains unclear. In this study we demonstrate that IL-27 inhibits CD28-mediated IL-2 production and that suppressor of cytokine signaling 3 (SOCS3) plays a critical role in the inhibitory effect. Although IL-27 enhanced IFN-γ production from naive CD4$^+$ T cells stimulated with plate-coated anti-CD3 and anti-CD28 in the presence of IL-12, IL-27 simultaneously inhibited CD28-mediated IL-2 production. Correlated with the inhibition, IL-27 was shown to augment SOCS3 expression. Analyses using various mice lacking a signaling molecule revealed that the inhibition of IL-2 production was dependent on STAT1, but not on STAT3, STAT4, and T-bet, and was highly correlated with the induction of SOCS3 expression. Similar inhibition of CD28-mediated IL-2 production and augmentation of SOCS3 expression by IL-27 were observed in a T cell hybridoma cell line, 2B4. Forced expression of antisense SOCS3 or dominant negative SOCS3 in the T cell line blocked the IL-27-inudced inhibition of CD28-mediated IL-2 production. Furthermore, pretreatment with IL-27 inhibited IL-2-mediated cell proliferation and STAT5 activation, although IL-27 hardly affected the induction level of CD25 expression. These results suggest that IL-27 inhibits CD28-mediated IL-2 production and also IL-2 responses, and that SOCS3, whose expression is induced by IL-27, plays a critical role in the inhibitory effect in a negative feedback mechanism. ***The Journal of Immunology,*** **2006, 176: 2773–2780.**

Interleukin-27 is a novel member of the IL-6/IL-12 family that consists of an IL-12 p40-related protein, EBV-induced gene 3, and a newly discovered IL-12 p35-related protein, p28 (1). The orphan cytokine receptor WSX-1/T cell cytokine receptor (TCCR),[3] which is homologous to the IL-12Rβ2 subunit, and gp130 constitute a functional signal-transducing receptor for IL-27 (1, 2). IL-27 activates JAK1, JAK2, TYK2, STAT1, STAT2, STAT3, STAT4, and STAT5 in naive CD4$^+$ T cells (3–6) and enhances proliferation in naive, but not memory, CD4$^+$ T cells. IL-27 also induces the expression of T-bet, a master transcriptional regulator for Th1 differentiation (7), and subsequent IL-12Rβ2 and synergizes with IL-12 in primary IFN-γ production (1, 3, 4, 6).

Previous studies using mice lacking one subunit of IL-27R, TCCR (8)/WSX-1 (9), revealed that IL-27 is required for the early initiation of Th1 responses, and that WSX-1/TCCR-deficient mice have enhanced susceptibility to infection with intracellular pathogens such as *Leishmania major* (9, 10) and *Listeria monocytogenes* (8). However, WSX-1 is not essential to develop the protective Th1 responses against *Toxoplasma gondii* parasites, but, rather, acts to attenuate the inflammatory responses induced by the protozoan infection, including cellular hyperactivation and overproduction of proinflammatory cytokines such as IFN-γ, IL-4, TNF-α, and IL-6 (5). In vitro analyses of the effect of IL-27 on Th1/Th2 differentiation demonstrated that IL-27 is not able to synergize with IL-12 to increase the production of IFN-γ by Th1 cells (11). Recent analyses of in vitro Th1/Th2 differentiation have revealed that the ability of IL-27 to induce Th1 differentiation is most prominent under Th1-polarizing conditions, but without IL-12, and is overruled by IL-12 (12). The IL-27-induced Th1 differentiation is mainly mediated by rapid and marked up-regulation of ICAM-1 expression on naive CD4$^+$ T cells through ICAM-1/LFA-1 interaction in a STAT1-dependent, but T-bet-, IFN-γ-, and STAT4-independent, mechanism. In contrast, it was recently demonstrated that IL-27 inhibits in vitro production of TNF and IL-12p40 in activated peritoneal macrophages from *WSX-1*$^{+/+}$ mice, but not from *WSX-1*$^{-/-}$ mice. Taken together, these in vivo and in vitro results indicate that IL-27 not only plays a role in the early regulation of Th1 differentiation, but also exerts an inhibitory effect on immune responses, including the suppression of proinflammatory cytokine production. However, the molecular mechanism by which IL-27 exerts the inhibitory effect remains unclear.

In the present study, we have found that IL-27 inhibits CD28-mediated IL-2 production in CD4$^+$ T cells and also IL-2 responses, and that suppressor of cytokine signaling (SOCS3), whose expression is induced by IL-27, mediates the inhibitory effect. Thus, IL-27, which is rapidly produced from APC by the interaction with T cells in the presence of Ag through CD40/CD40L interaction (1), plays important roles not only to augment

*Intractable Immune System Disease Research Center, Tokyo Medical University, Shinjuku, Tokyo, Japan; †Department of Patho-Physiology, Faculty of Pharmaceutical Sciences, Tokyo University of Science, Chiba, Japan; ‡Department of Immunology, Tokyo Medical University, Tokyo, Japan; §Department of Clinical Sciences, Faculty of Pharmaceutical Sciences, Josai International University, Chiba, Japan; and ¶Department of Molecular Genetics, Medical Institute of Bioregulation, Kyushu University, Fukuoka, Japan

Received for publication July 13, 2005. Accepted for publication December 29, 2005.

The costs of publication of this article were defrayed in part by the payment of page charges. This article must therefore be hereby marked *advertisement* in accordance with 18 U.S.C. Section 1734 solely to indicate this fact.

[1] This study was supported by Grant-in-Aid for Scientific Research, High-Tech Research Center Project, and University-Industry Joint Research Project from the Ministry of Education, Culture, Sports, Science, and Technology of Japan and a grant from Novartis Foundation (Japan) for the Promotion of Science.

[2] Address correspondence and reprint requests to Dr. Takayuki Yoshimoto, Intractable Immune System Disease Research Center, Tokyo Medical University, 6-1-1 Shinjuku, Shinjuku-ku, Tokyo 160-8402, Japan. E-mail address: yoshimot@tokyo-med.ac.jp

[3] Abbreviations used in this paper: TCCR, T cell cytokine receptor; HPRT, hypoxanthine phosphoribosyltransferase; pY, phosphotyrosine; SOCS, suppressor of cytokine signaling; Tg, transgenic.

0022-1767/06/$02.00

T cell proliferation by itself and regulate early Th1 differentiation, but also to suppress excessive progression of CD28-mediated IL-2 production and IL-2 responses by inducing SOCS3 expression in a negative feedback mechanism.

Materials and Methods

Mice

BALB/c mice were purchased from Japan SLC. Mice transgenic (Tg) for $\alpha\beta$ TCR recognizing $OVA_{323-339}$ (DO11.10; BALB/c background) (13) were provided by Dr. T. Yoshimoto (Hyogo College of Medicine, Hyogo, Japan). *STAT1*$^{+/-}$ and *STAT1*$^{-/-}$ mice (14) of a mixed background of 129/Sv and C57BL/6 were provided by Dr. R. D. Schreiber (Washington University, St. Louis, MO). STAT1-deficient mice (14) of 129/Sv background and wild-type 129/Sv mice were purchased from Taconic Farms. Mice lacking STAT3 specifically in T cells (Lck-Cre/*STAT3*$^{flox/flox}$) were generated by mating *STAT3*$^{flox/flox}$ mice (15), in which the STAT3 gene is flanked by two loxP sites, and Lck-Cre Tg mice (16) (purchased from Center for Animal Resources and Development), in which the Cre recombinase transgene is regulated by T cell-specific Lck promoter. *STAT3*$^{flox/flox}$, Lck-Cre/*STAT3*$^{flox/+}$, or Lck-Cre/*STAT3*$^{+/+}$ mice were used as control mice. STAT4-deficient mice (17) and T-bet-deficient mice (18) of BALB/c background were purchased from The Jackson Laboratory. All animal experiments were performed in accordance with our institutional guidelines.

Cells

Naive CD4$^+$ T cells and a mouse T cell hybridoma cell line 2B4, provided by Dr. T. Saito (RIKEN Research Center for Allergy and Immunology, Kanagawa, Japan), were cultured in RPMI 1640 medium supplemented with 10% FBS and 50 μM 2-ME. PLAT-E, a packaging cell line provided by Dr. T. Kitamura (University of Tokyo, Tokyo, Japan) (19), was maintained in DMEM supplemented with 10% FBS.

Reagents

Anti-CD3 (145-2C11), anti-IL-2 (S4B6), anti-IL-4 (11B11), anti-IFN-γ (XMG1.2), and anti-Thy1.2 (30-H12) were purchased from American Type Culture Collection. Anti-CD28 (37.51) and mouse rIL-2 were obtained from BD Biosciences. Anti-CD25 (PC61.5) and FITC-anti-rat IgG were obtained from eBioscience. Anti-STAT1, anti-STAT3, anti-STAT5, and T-bet were purchased from Santa Cruz Biotechnology. Anti-phosphotyrosine (anti-pY)-STAT1, anti-pY-STAT3, and anti-pY-STAT5 were obtained from Cell Signaling Technology. Anti-SOCS3 and anti-actin were purchased from Medical Biological Laboratories and Sigma-Aldrich, respectively. Mouse rIL-12 was obtained from R&D Systems. Human rIL-2 and mouse rIFN-γ were provided by Shionogi.

Preparation of purified rIL-27 protein

Recombinant IL-27 was prepared as a soluble tagged fusion protein by flexibly linking EBV-induced gene 3 to p28 as described previously (20).

Preparation of naive CD4$^+$ T cells

Primary T cells were purified by passing spleen cells depleted of erythrocytes through nylon wool. The flow-through fraction was incubated with biotin-conjugated anti-CD8α, anti-B220, anti-Mac-1, anti-Ter-119, and anti-DX5, followed by incubation with anti-biotin magnetic beads (Miltenyi Biotec) and passed through a magnetic cell sorting column (Miltenyi Biotec); the negative fraction was collected (CD4$^+$ T cells, >95%). These purified T cells were then incubated with anti-CD62L magnetic beads (Miltenyi Biotec), and the positive fraction was collected as purified naive CD4$^+$ T cells (CD62L$^+$ cells, >99%).

IL-2 and IFN-γ production assays

Naive CD4$^+$ T cells (1×10^5 cells/ml) from DO11.10 Tg mice were stimulated with 1 μM $OVA_{323-339}$ peptide and irradiated T/NK cell-depleted BALB/c spleen cells (1×10^6 cells/ml) in the presence or the absence of IL-27 (10 ng/ml) for various times. T/NK cell-depleted spleen cells were prepared as follows. Spleen cells depleted of erythrocytes were incubated with anti-Thy1.2, followed by incubation with anti-rat IgG magnetic beads (Miltenyi Biotec) together with anti-DX5 magnetic beads (Miltenyi Biotec) and passed through a magnetic cell-sorting column. The negative fraction was used as T/NK cell-depleted spleen cells. Naive CD4$^+$ T cells (5×10^5 cells/ml) were stimulated with plate-coated anti-CD3 (2 μg/ml) and anti-CD28 (0.5 μg/ml) in the presence or the absence of IL-27 and/or IL-12 (10 ng/ml) for various times. 2B4 cells (2×10^5 cells/ml) were stimulated with plate-coated anti-CD3 (0.03 μg/ml) and anti-CD28 (0.5 μg/ml) in the presence or the absence of IL-27 for 16 h. Culture supernatant was collected and analyzed for IL-2 and/or IFN-γ production by ELISA (21).

RT-PCR analysis

Total RNA was extracted by using a guanidine thiocyanate procedure, cDNA was prepared using oligo(dT) primer and SuperScript reverse transcriptase (Invitrogen Life Technologies), and RT-PCR was performed using *Taq* DNA polymerase as described previously (22). Cycle conditions were 94°C for 40 s, 60°C for 20 s, and 72°C for 40 s. Primers used for hypoxanthine phosphoribosyltransferase (HPRT) were described previously (23). The following primers were also used; SOCS3 sense primer, 5′-TTGTCGGAAGACTGTCAACG-3′; SOCS3 antisense primer, 5′-GAGAGTCCGCTTGTCAAAGG-3′; WSX-1 sense primer, 5′-ACCCAAA TGAAGCCAGACAC-3′; WSX-1 antisense primer, 5′-CACACAAGGT CTTGGGTCCT-3′; gp130 sense primer, 5′-AGTCTGGGTGGAAGCA GAGA-3′; and gp130 antisense primer, 5′-CTTGGTGGTCTGGA TGGTCT-3′.

Quantitative RT-PCR analysis

cDNA synthesis was performed as described above. Real-time PCR was performed on an ABI 7500 (Applied Biosystems). PCR primers and probes for mouse SOCS3 and HPRT in the TaqMan Rodent Control Reagents and TaqMan Gene Expression Assays (Applied Biosystems), respectively, were used according to the manufacturer's instructions. PCR parameters are as recommended for the TaqMan Universal PCR Master Mix kit (Applied Biosystems). Triplicate samples of 2-fold serial dilutions of cDNA were assayed and used to construct the standard curves.

Preparation of 2B4 transfectants

SOCS3 cDNA was isolated by RT-PCR using total RNA prepared from Con A-activated spleen cells and was confirmed by sequencing. Antisense SOCS3 cDNA (24) was generated using standard PCR methods and subcloned into p3xFLAG-CMV-10 vector (Sigma-Aldrich). 2B4 cells were then transfected with the antisense SOCS3 expression vector or the empty vector as a control by electroporation and selected with geneticin (G418).

Retroviral infection

Wild-type SOCS3, dominant-negative SOCS3(F25A) (25, 26), and antisense SOCS3 cDNAs were generated using standard PCR methods and subcloned into a bicistronic retroviral vector pMX-IRES/EGFP (27), provided by Dr. T. Kitamura. The PLAT-E cell line was transfected with the resultant vectors or the empty vector as control by using FuGene 6 (Roche) and cultured to generate the retroviral supernatant. 2B4 cells were then infected with the supernatant as described previously (28) and purified by sorting using a FACSVantage (BD Biosciences).

Proliferation assay

Naive CD4$^+$ T cells (1×10^6 cells/ml) were stimulated with plate-coated anti-CD3 (2 μg/ml) and anti-CD28 (0.5 μg/ml) in the presence or the absence of IL-27. After 3 days, stimulated cells were recovered and washed. Resultant cells (1×10^5 cells/ml) were cultured in the presence of human IL-2 for 48 h and pulsed with [^{3}H]thymidine for the last 24 h.

Western blotting

Cells were lysed in a lysis buffer containing protease inhibitors, and resultant cell lysates were separated by SDS-PAGE under reducing conditions and transferred to polyvinylidene difluoride membrane (Millipore) as described previously (28). The membrane was blocked, probed with primary Ab and then with the appropriate secondary Ab conjugated to HRP, and visualized with the ECL detection system (Amersham Biosciences) according to the manufacturer's instructions.

Results

IL-27 inhibits CD28-mediated IL-2 production in naive CD4$^+$ T cells stimulated with Ag plus APC and also with plate-coated anti-CD3 plus anti-CD28

We and other groups previously reported that IL-27 induces T-bet and subsequent IL-12β2 expression in naive CD4$^+$ T cells and synergizes with IL-12 in IFN-γ production (1, 3, 4, 6). Although T-bet transcriptionally up-regulates IFN-γ production, it was originally demonstrated to down-regulate IL-2 production as well (7).

In addition, WSX-1-deficient CD4$^+$ T cells were reported to overproduce IL-2 (5). Therefore, we first examined the effect of IL-27 on primary IL-2 production. Naive CD4$^+$ T cells from DO11.10 Tg mice were stimulated with $OVA_{323-339}$ peptide and irradiated T/NK cell-depleted BALB/c spleen cells in the presence or the absence of IL-27 (10 ng/ml) for various times, and culture supernatant was collected and analyzed for IL-2 production by ELISA. The Ag-specific IL-2 production in naive CD4$^+$ T cells gradually increased with time, and IL-27 greatly inhibited IL-2 production (Fig. 1*A*). Furthermore, naive CD4$^+$ T cells from wild-type BALB/c mice were stimulated with plate-coated anti-CD3 and anti-CD28 in the presence of IL-27 and/or IL-12 for various times and analyzed for IL-2 and IFN-γ production (Fig. 1, *B* and *C*). As reported previously (1, 3, 4, 6), IL-27 induced T-bet expression (data not shown) and synergistic IFN-γ production with IL-12 (Fig. 1*C*). In marked contrast, IL-27 clearly inhibited IL-2 production in a dose-dependent manner, whereas IL-12 failed to affect IL-2 production, but appeared to enhance the inhibitory effect of IL-27 (Fig. 1, *B* and *D*). Without costimulation by anti-CD28, IL-2 production was not detected under the experimental conditions (Fig. 1*E*). In the presence of anti-CD28, greater production of IL-2 was observed with the higher dose of anti-CD3 used for plate coating. IL-27 inhibited IL-2 production independently of the dose of anti-CD3. These results suggest that IL-27 inhibits CD28-mediated IL-2 production in naive CD4$^+$ T cells stimulated with Ag plus APC and also with plate-coated anti-CD3 plus anti-CD28.

IL-27 induces SOCS3 expression in naive CD4$^+$ T cells stimulated with plate-coated anti-CD3 and anti-CD28

Recently, it was reported that the expression of SOCS3 in early T cell activation influences the ability of IL-2 production mediated by CD28 costimulation (25). In addition, IFN-γ and IL-6 activate STAT1 and STAT3, respectively, both of which lead to SOCS3 induction. Therefore, we next examined the effect of IL-27 on SOCS3 expression. Naive CD4$^+$ T cells were stimulated with plate-coated anti-CD3 and anti-CD28 in the presence or the absence of IL-27 for various times, total RNA was prepared and analyzed for SOCS3 and HPRT mRNA expression by RT-PCR and real-time PCR (Fig. 2). As reported previously (25), primary unstimulated CD4$^+$ T cells expressed a significant level of SOCS3 mRNA, and the expression rapidly decreased after stimulation. However, in the presence of IL-27, SOCS3 expression was quickly recovered and increased; this pattern appeared to correlate with the inhibition of IL-2 production (Fig. 1*B*). These results suggest that IL-27 induces SOCS3 expression in naive CD4$^+$ T cells stimulated with plate-coated anti-CD3 and anti-CD28, implying that SOCS3 may play a role in the exertion of inhibitory effects by IL-27.

STAT1, but not STAT3, STAT4, and T-bet, is required for the inhibition of CD28-mediated IL-2 production by IL-27, which is highly correlated with the induction of SOCS3 expression

To further explore the correlation between inhibition of IL-2 production and induction of SOCS3 expression by IL-27 and also which IL-27 downstream signaling molecule is required for the inhibition of CD28-mediated IL-2 production, we next used various mice lacking each of these signaling molecules, T-bet, STAT1, STAT3, and STAT4. Naive CD4$^+$ T cells were prepared from these knockout mice and respective control mice and stimulated with plate-coated anti-CD3 and anti-CD28 in the presence or the absence of IL-27. After 48 h, culture supernatant was collected and analyzed for IL-2 production by ELISA. Total RNA was also prepared and analyzed for SOCS3 and HPRT mRNA expression by

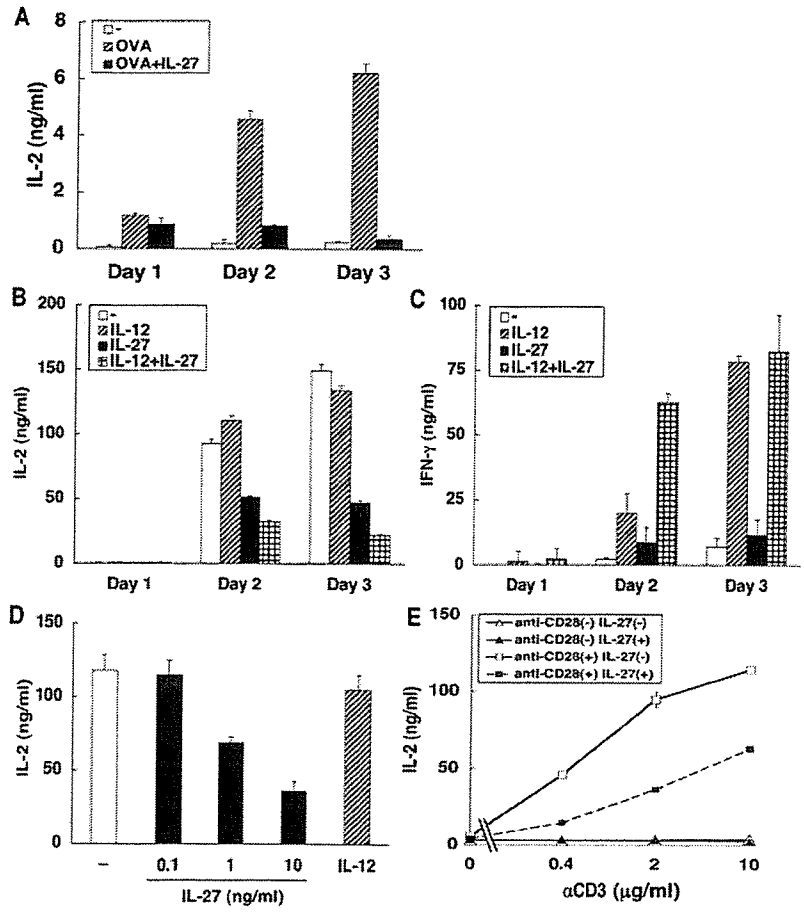

FIGURE 1. IL-27 inhibits CD28-mediated IL-2 production in naive CD4$^+$ T cells stimulated with Ag plus APC and also with plate-coated anti-CD3 plus anti-CD28. *A*, Inhibition of Ag-specific IL-2 production by IL-27. Naive CD4$^+$ T cells from DO11.10 Tg mice were stimulated with $OVA_{323-339}$ peptide and irradiated T/NK cell-depleted BALB/c spleen cells in the presence or the absence of IL-27 (10 ng/ml) for various times. *B* and *C*, Inhibition of IL-2 production, but augmentation of IFN-γ production in the presence of IL-12 by IL-27. Naive CD4$^+$ T cells were stimulated with plate-coated anti-CD3 and anti-CD28 in the presence or the absence of IL-27 (10 ng/ml) and/or IL-12 (10 ng/ml) for various times. *D*, Dose-dependent inhibition of IL-2 production by IL-27. Naive CD4$^+$ T cells were stimulated with plate-coated anti-CD3, anti-CD28, and various concentrations of IL-27 for 48 h. *E*, Inhibition of IL-2 production by IL-27 independently of the dose of anti-CD3 used for plate coating. Naive CD4$^+$ T cells were stimulated with various doses of plate-coated anti-CD3 and IL-27 (10 ng/ml) in the presence or the absence of anti-CD28 for 48 h. Culture supernatant was collected and assayed for IL-2 and/or IFN-γ production in triplicate by ELISA. Data are shown as the mean ± SD. Similar results were obtained in three to five independent experiments.

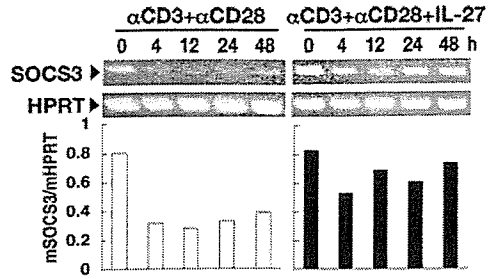

FIGURE 2. IL-27 induces SOCS3 expression in naive $CD4^+$ T cells stimulated with plate-coated anti-CD3 and anti-CD28. Naive $CD4^+$ T cells were stimulated with plate-coated anti-CD3 and anti-CD28 in the presence or the absence of IL-27 (10 ng/ml) for various times. Total RNA was prepared and analyzed for mRNA expression of SOCS3 and HPRT as a control by RT-PCR and real-time PCR. Similar results were obtained in six independent experiments.

RT-PCR. Inhibition of IL-2 production by IL-27 was still observed in STAT3-, STAT4-, and T-bet-deficient naive $CD4^+$ T (Fig. 3, *B–D*). However, in *STAT1*$^{-/-}$ naive $CD4^+$ T cells, IL-2 production was hardly inhibited by IL-27 compared with that in *STAT1*$^{+/-}$ naive $CD4^+$ T cells (Fig. 3*A*). Consistent with these results, the induction of SCOS3 mRNA expression was still observed in STAT3-, STAT4-, and T-bet-deficient naive $CD4^+$ T cells, but not in STAT1-deficient naive $CD4^+$ T cells (Fig. 3). These results suggest that the inhibition of IL-2 production is highly correlated with the induction of SOCS3 expression, and that STAT1 is required for inhibition of CD28-mediated IL-2 production and induction of SOCS3 expression by IL-27, although STAT3, STAT4, and T-bet are not essential to them.

Similar inhibition of IL-2 production and induction of SOCS3 expression by IL-27 are observed in a T cell hybridoma cell line 2B4 as well as in primary naive $CD4^+$ T cells

To clarify a role for SOCS3 in the inhibition of CD28-mediated IL-2 production by IL-27, we next used a $CD4^+$ T cell hybridoma cell line, 2B4, instead of primary naive $CD4^+$ T cells. We first confirmed that 2B4 cells express both IL-27R subunits, gp130 and WSX-1, which were determined by RT-PCR (data not shown), and that 2B4 cells are responsive to IL-27, resulting in activation of STAT1 and STAT3, which was detected by Western blotting using anti-pY-STAT1 and anti-pY-STAT3 (data not shown). Then, 2B4 cells were stimulated with plate-coated anti-CD3 and anti-CD28 in the presence of IL-27. Culture supernatant was collected after 16 h and analyzed for IL-2 production by ELISA (Fig. 4*A*). Although stimulation with plate-coated anti-CD3 alone induced the production of significant amounts of IL-2, the addition of anti-CD28 further enhanced IL-2 production. Consistent with the results obtained using primary naive $CD4^+$ T cells (Fig. 1*D*), IL-27 efficiently inhibited the CD28-mediated IL-2 production to the level obtained after stimulation with plate-coated anti-CD3 alone in a dose-dependent manner. Moreover, total RNA was prepared after the 3-h stimulation and analyzed for mRNA expression of SOCS3 by RT-PCR and real-time PCR (Fig. 4*B*). Correlated with the inhibition of IL-2 production, SOCS3 mRNA expression was induced in the presence of IL-27. Thus, the inhibition of CD28-mediated IL-2 production and the induction of SOCS3 expression

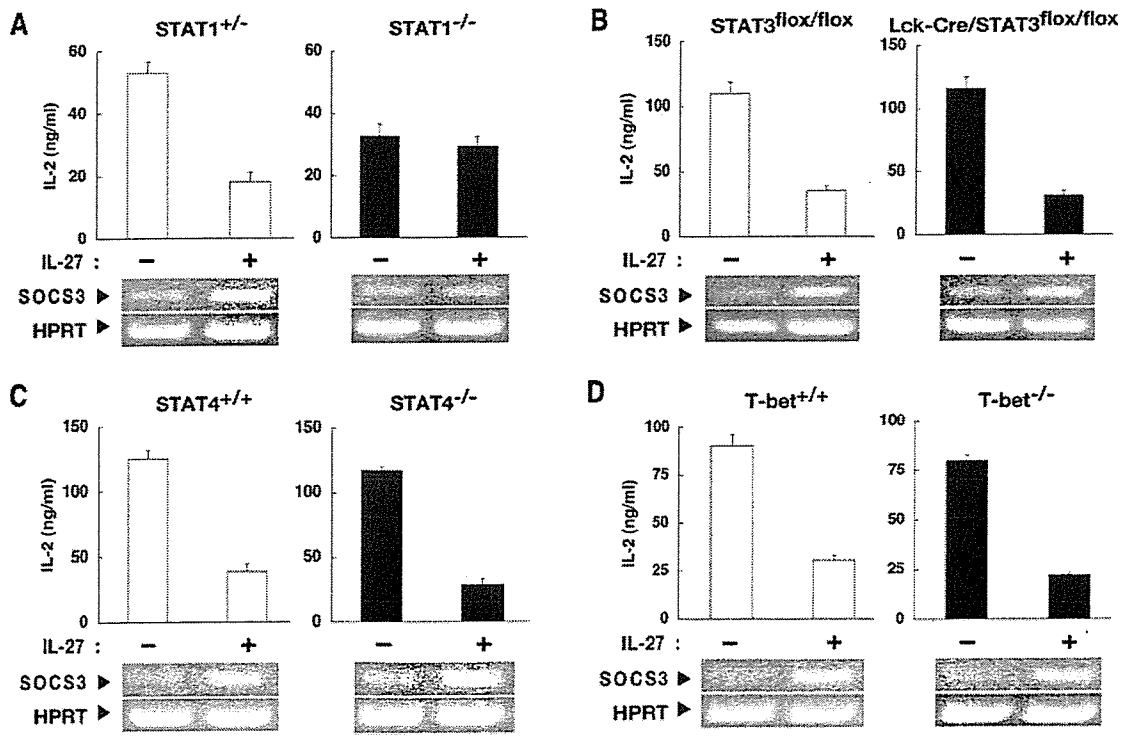

FIGURE 3. STAT1, but not STAT3, STAT4, or T-bet, is required for the inhibition of CD28-mediated IL-2 production by IL-27, which is highly correlated with the augmentation of SOCS3 expression. Naive $CD4^+$ T cells lacking each of the IL-27 downstream signaling molecules, STAT1 (*A*), STAT3 (*B*), STAT4 (*C*), and T-bet (*D*), and their control cells were stimulated with plate-coated anti-CD3 and anti-CD28 in the presence or the absence of IL-27 (10 ng/ml) for 48 h. Culture supernatant was collected and assayed for IL-2 production in triplicate by ELISA. Data are shown as the mean ± SD. Total RNA was also prepared and analyzed for mRNA expression of SOCS3 and HPRT as a control by RT-PCR. Similar results were obtained in at least three independent experiments.

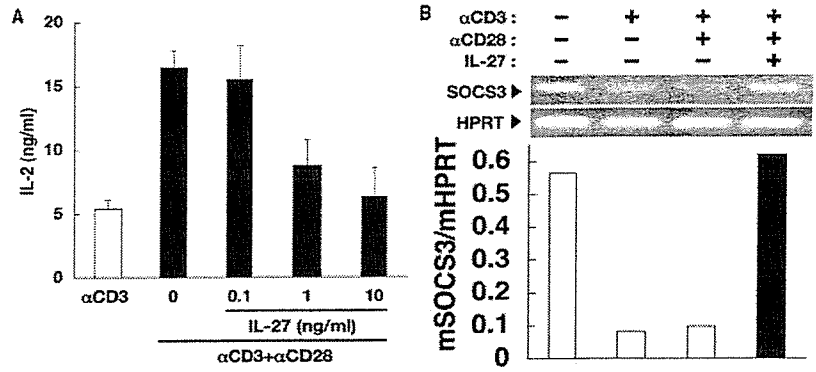

FIGURE 4. Similar inhibition of IL-2 production and augmentation of SOCS3 expression by IL-27 are observed in a T cell hybridoma cell line 2B4 as well as in primary naive $CD4^+$ T cells. *A*, 2B4 cells were stimulated with plate-coated anti-CD3 and anti-CD28 in the presence or the absence of various concentrations of IL-27 for 16 h. Culture supernatant was then collected and assayed for IL-2 production in triplicate by ELISA. Data are shown as the mean ± SD. *B*, Total RNA was also prepared after the stimulation for 3 h in the presence or the absence of IL-27 (10 ng/ml) and was analyzed for mRNA expression of SOCS3 and HPRT as a control by RT-PCR and real-time *PCR*. Similar results were obtained in at least three independent experiments.

by IL-27 were observed not only in primary naive $CD4^+$ T cells, but also in a T cell hybridoma cell line, 2B4.

Forced expression of antisense SOCS3 or dominant negative SOCS3(F25A) in a T cell line blocks the inhibition of CD28-mediated IL-2 production by IL-27

Because a T cell line is more suitable for gene transduction, we next generated 2B4 cells devoid of functional SOCS3 expression by transducing antisense SOCS3 or dominant negative SOCS3(F25A). We first prepared 2B4 cells expressing antisense SOCS3 and its empty vector as a control by transfecting and selection with geneticin (G418). Resultant stable transfectants (two clones each) were then stimulated with plate-coated anti-CD3 and anti-CD28 in the presence or the absence of IL-27. After stimulation for 3 h, total RNA was prepared and analyzed for mRNA expression of SOCS3 by RT-PCR. Augmentation of SOCS3 mRNA expression by IL-27 was barely observed in 2B4 transfectants expressing antisense SOCS3, although augmentation was clearly observed in 2B4 transfectants expressing control vector (Fig. 5*A*). Correlated with the inability to augment SOCS3 mRNA expression, inhibition of IL-2 production by IL-27 was not detected in 2B4 transfectants expressing antisense SOCS3, although the inhibition was clearly detected in 2B4 transfectants expressing control vector (Fig. 5*A*).

We also prepared 2B4 cells expressing dominant negative SOCS3(F25A), which contains a point mutation in the kinase inhibitory region of SOCS3 (25, 26), antisense SOCS3, and control vector by retrovirus-mediated gene transduction, followed by purification with sorting, and analyzed the ability of IL-27 to inhibit CD28-mediated IL-2 production in these 2B4 cells as described above. The expression of dominant negative SOCS3(F25A) and wild-type SOCS3 was confirmed by Western blotting using anti-SOCS3, although endogenous expression of SOCS3 was hardly

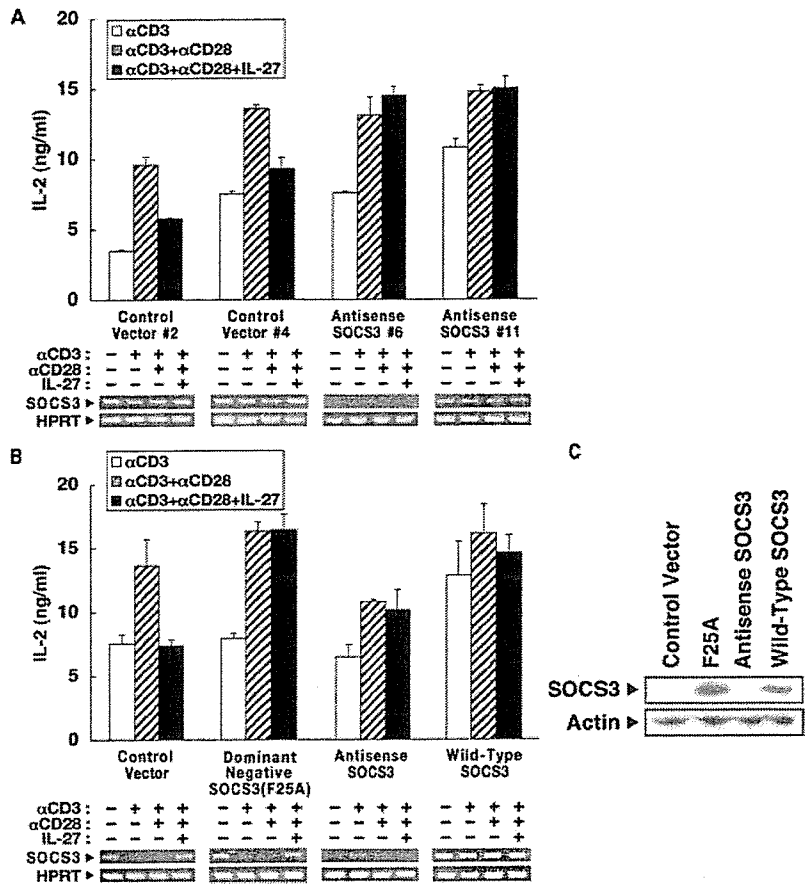

FIGURE 5. Forced expression of antisense SOCS3 or dominant negative SOCS3(F25A) in a T cell line blocks the inhibition of CD28-mediated IL-2 production by Il-27. 2B4 stable transfectants (two clones each) expressing antisense SOCS3 or control vector (*A*), and 2B4 cells, expressing dominant negative SOCS3(F25A), antisense SOCS3, wild-type SOCS3, or control vector (*B*), which were prepared by retrovirus-mediated gene transduction, were stimulated with plate-coated anti-CD3 and anti-CD28 in the presence or the absence of IL-27 (10 ng/ml) for 16 h. Culture supernatant was then collected and assayed for IL-2 production in triplicate by ELISA. Data are shown as the mean ± SD. Total RNA was also prepared after the stimulation for 3 h and was analyzed for mRNA expression of SOCS3 and HPRT as a control by RT-PCR. Expression of SOCS3 at the protein level in these unstimulated cells was analyzed by Western blotting with anti-SOCS3 and anti-actin (*C*). Similar results were obtained in at least three independent experiments.

detected (Fig. 5*C*). Augmentation of SOCS3 mRNA by IL-27 was observed in 2B4 cells expressing control vector and dominant negative SOCS3(F25A), although almost no augmentation of SOCS3 mRNA expression was observed in 2B4 cells expressing antisense SOCS3 (Fig. 5*B*). Constitutive expression of SOCS3 mRNA was observed in 2B4 cells expressing wild-type SOCS3. In 2B4 cells expressing dominant negative SOCS3(F25A) and antisense SOCS3, but not in those expressing control vector, CD28-mediated IL-2 production was hardly inhibited by IL-27. In contrast, in 2B4 cells expressing wild-type SOCS3, augmentation of IL-2 production by anti-CD28 itself was not observed regardless of the presence or the absence of IL-27.

Taken together, these results suggest that IL-27 inhibits CD28-mediated IL-2 production, and that SOCS3, whose expression is induced by IL-27, plays a critical role in the inhibitory effect.

IL-27 inhibits IL-2-mediated cell proliferation and STAT5 activation without affecting CD25 expression

When naive $CD4^+$ T cells were stimulated with plate-coated anti-CD3 and anti-CD28 in the presence or the absence of IL-27 for 3 days and then expanded in medium containing IL-2 for 3 more days, we initially noticed that recovery of the cell number in the presence of IL-27 appears to be less than that in the absence of IL-27 (data not shown). This implies that IL-27 may affect IL-2-mediated cell proliferation in addition to IL-2 production. Therefore, we finally investigated the effect of pretreatment with IL-27 on IL-2 responses. Naive $CD4^+$ T cells were stimulated with plate-coated anti-CD3 and anti-CD28 in the presence or the absence of IL-27 for 3 days, and then these cells were washed and analyzed for the responsiveness to IL-2 by determining IL-2-mediated cell proliferation and tyrosine phosphorylation of STAT5, which is a critical signaling molecule activated by IL-2 (Fig. 6, *A* and *B*, respectively). Naive $CD4^+$ T cells stimulated in the absence of IL-27 efficiently proliferated in response to increasing amounts of IL-2. In contrast, pretreatment with IL-27 reduced IL-2-mediated cell proliferation dose-dependently. The pretreatment also inhibited IL-2-induced STAT5 phosphorylation in *STAT1*$^{+/+}$ naive $CD4^+$ T cells, but not in *STAT1*$^{-/-}$ naive $CD4^+$ T cells. This is consistent with the finding that STAT1 is required for induction of SOCS3 expression by IL-27 (Fig. 3). We then examined the effect of IL-27 on the induction of CD25 (IL-2Rα) expression by FACS analysis. Stimulation with plate-coated anti-CD3 and anti-CD28 greatly enhanced CD25 expression on naive $CD4^+$ T cells, whereas comparable induction of CD25 expression was observed in the presence and the absence of IL-27 (Fig. 6*C*). These results suggest that IL-27 inhibits IL-2-mediated cell proliferation and STAT5 activation without affecting CD25 expression as well as IL-2 production.

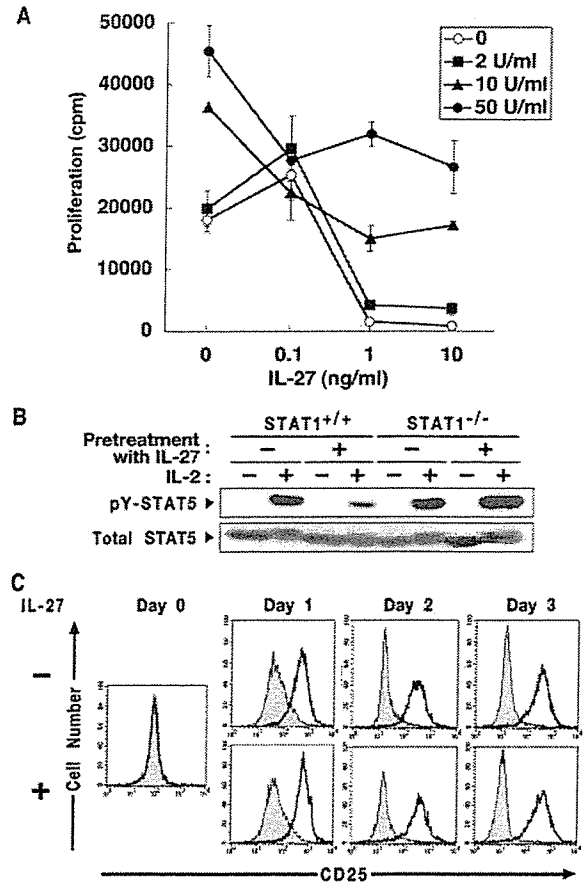

FIGURE 6. IL-27 inhibits IL-2-mediated cell proliferation and STAT5 activation without affecting CD25 expression. *A*, Inhibition of IL-2-mediated proliferation by pretreatment with IL-27. Naive $CD4^+$ T cells were stimulated with plate-coated anti-CD3 and anti-CD28 in the presence of various concentrations of IL-27 for 3 days, then these cells were washed and analyzed for the responsiveness to IL-2 by measuring IL-2-mediated proliferation. Cells were restimulated with various concentrations of human IL-2 for 48 h and were pulsed with [^{3}H]thymidine for the last 24 h. *B*, Inhibition of IL-2-induced STAT5 activation by pretreatment with IL-27. *STAT1*$^{+/+}$ and *STAT1*$^{-/-}$ (129/Sv background) naive $CD4^+$ T cells were stimulated with plate-coated anti-CD3 and anti-CD28 in the presence of IL-27 (10 ng/ml) for 3 days, then these cells were washed, rested overnight, and restimulated with mouse IL-2 (10 ng/ml) for 20 min. STAT5 activation was analyzed by Western blotting with anti-pY-STAT5 and anti-total STAT5. *C*, No effect of IL-27 on up-regulation of CD25 expression. Naive $CD4^+$ T cells were stimulated with plate-coated anti-CD3 and anti-CD28 in the presence or the absence of IL-27 (10 ng/ml) for various times and analyzed for cell surface expression of CD25 by FACS using anti-CD25 (solid line) and control rat IgG (plain line with shading). Similar results were obtained in at least two independent experiments.

Discussion

Although IL-27 has both immune stimulatory and inhibitory effects, the molecular mechanism by which IL-27 exerts the inhibitory effect remains unclear. In the present study, we have elucidated that IL-27 induces SOCS3 expression, which plays a critical role in the inhibitory effect, including inhibition of CD28-mediated IL-2 production (Figs. 1–5). This is consistent with the previous report showing that WSX-1-deficient $CD4^+$ T cells overproduce IL-2 (5). Induction of SOCS3 expression by IL-27 is mediated through the activation of STAT1, but not of STAT3, STAT4, and T-bet (Fig. 3). Moreover, IL-27 also inhibits IL-2-mediated cell proliferation and STAT5 activation without affecting CD25 expression (Fig. 6), presumably through SOCS3. T-bet is a potent transactivator of the IFN-γ gene and a master transcriptional regulator for Th1 differentiation, whereas it simultaneously represses IL-2 gene transcription (7). IL-27 can augment T-bet and subsequent IL-12Rβ2 expression in naive $CD4^+$ T cells, resulting in synergistic IFN-γ production with IL-12 (1, 3, 4, 6). Therefore, we initially expected that T-bet might be required for the inhibition of IL-2 production by IL-27. However, it turned out that SOCS3, but not T-bet, is required for the inhibition of IL-2 production (Fig. 3). Moreover, it was recently demonstrated that SOCS3 expression induced by IFN-γ is achieved via activation of STAT1, but not STAT3 (29). Similarly, IL-27 was revealed to induce SOCS3 expression via activation of STAT1, but not STAT3 (Fig. 3), although IL-27 can activate both STAT1 and STAT3 efficiently (3–6).

Previously, it was demonstrated that SOCS3 is rapidly induced by IL-2 in T cells and inhibits IL-2 responses, including STAT5